

Optical imaging for the *Spitzer* Survey of Stellar Structure in Galaxies[★]

Data release and notes on interacting galaxies

Johan H. Knapen^{1,2}, Santiago Erroz-Ferrer^{1,2}, Javier Roa^{1,3}, Judit Bakos^{1,2,4}, Mauricio Cisternas^{1,2}, Ryan Leaman^{1,2}, and Nik Szymanek⁵

¹ Instituto de Astrofísica de Canarias, E-38200 La Laguna, Spain; e-mail: jhk@iac.es

² Departamento de Astrofísica, Universidad de La Laguna, E-38206 La Laguna, Spain

³ Space Dynamics Group, Universidad Politécnica de Madrid, E-28040 Madrid, Spain

⁴ Konkoly Observatory, Research Centre for Astronomy and Earth Sciences, Hungarian Academy of Sciences, Konkoly Thege Miklós út 15-17, H-1121 Budapest, Hungary

⁵ 186 Thorndon Avenue, West Horndon, Essex, CM13 3TP, UK

Received; accepted 3 June 2014

ABSTRACT

Context. The *Spitzer* Survey for Stellar Structure in Galaxies (S⁴G) and its more recently approved extension will lead to a set of 3.6 and 4.5 μ m images for 2829 galaxies, which can be used to study many different aspects of the structure and evolution of local galaxies.

Aims. We have collected and re-reduced optical images of 1768 of the survey galaxies, aiming to make these available to the community as ready-to-use FITS files to be used in conjunction with the mid-IR images. Our sky-subtraction and mosaicking procedures were optimised for imaging large galaxies. We also produce false-colour images of some of these galaxies to be used for illustrative and public outreach purposes.

Methods. We collected and re-processed images in five bands from the Sloan Digital Sky Survey for 1657 galaxies, which are publicly released with the publication of this paper. We observed, in only the g-band, an additional 111 S⁴G galaxies in the northern hemisphere with the 2.5 m Liverpool Telescope, so that optical imaging is released for 1768 galaxies, or for 62% of the S⁴G sample. We visually checked all images. We noted interactions and close companions in our optical data set and in the S⁴G sample, confirming them by determining the galaxies' radial velocities and magnitudes in the NASA-IPAC Extragalactic Database.

Results. We find that 17% of the S⁴G galaxies (21% of those brighter than 13.5 mag) have a close companion (within a radius of five times the diameter of the sample galaxy, a recession velocity within $\pm 200 \text{ km s}^{-1}$ and not more than 3 mag fainter) and that around 5% of the bright part of the S⁴G sample show significant morphological evidence of an ongoing interaction. This confirms and further supports previous estimates of these fractions.

Conclusions. The over 8000 science images described in this paper, the re-processed Sloan Digital Sky Survey ones, the new Liverpool Telescope images, the set of 29 false-colour pictures, and the catalogue of companion and interacting galaxies, are all publicly released for general use for scientific, illustrative, or public outreach purposes.

Key words. Galaxies: structure - Galaxies: interactions - Surveys

1. Introduction

The *Spitzer* Survey of Stellar Structure in Galaxies (S⁴G; Sheth et al. 2010) has used the *Spitzer* Space Telescope Infrared Array Camera (IRAC; Fazio et al. 2004) at 3.6 and 4.5 μ m to observe the stellar mass distribution in a sample of 2352 galaxies¹. These bands are excellent tracers of the underlying stellar mass distribution, from which the gravitational potential can be derived, especially once they have been corrected for the limited contributions of young stars (e.g., Meidt et al. 2012; Eskew et al. 2012; Meidt et al. 2014, M. Querejeta et al. in preparation). A recently approved extension to the original S⁴G survey will add 477 galaxies² of predominantly early morphological types, for which 3.6 and 4.5 μ m are being obtained in the current Cycle 10 of *Spitzer* observations. This will bring the size of the combined S⁴G sample to a total of 2829 nearby galaxies, covering the whole sky, and selected using

[★]Tables 1 and 3 and FITS files of the images are available at the Centre de Données astronomiques de Strasbourg (CDS) via anonymous ftp to cdsarc.u-strasbg.fr (130.79.128.5) or via <http://cdsarc.u-strasbg.fr/viz-bin/qcat?J/A+A/xxx/yyy>. The images are also offered through the NASA/IPAC Extragalactic Database (NED).

¹ The size of the original S⁴G sample as described in Sheth et al. 2010 was 2331 galaxies, but we refer here to 2352 the galaxies actually observed in the survey and released through the NASA/IPAC Infrared Science Archive (IRSA).

² The sample of the S⁴G extension proposal for *Spitzer* has 695 galaxies, but 218 of these overlap with the original S⁴G.

Table 1. Details on optical images

Galaxy	PGC	Source	Bands	FOV [arcmin]	Calibration
UGC 12893	38	SDSS/DR8	<i>u, g, r, i, z</i>	5.0	-
NGC 7814	218	SDSS/DR7	<i>u, g, r, i, z</i>	13.1	-
UGC 00017	255	SDSS/DR7	<i>u, g, r, i, z</i>	7.3	-
NGC 7817	279	SDSS/DR8	<i>u, g, r, i, z</i>	9.9	-
NGC 0014	647	SDSS/DR7	<i>u, g, r, i, z</i>	5.0	-
UGC 00099	757	SDSS/DR8	<i>u, g, r, i, z</i>	7.5	-
UGC 00122	889	LT/RATCam	<i>g'</i>	4.6	1
UGC 00132	924	SDSS/DR8	<i>u, g, r, i, z</i>	5.0	-
UGC 00156	1107	SDSS/DR8	<i>u, g, r, i, z</i>	5.0	-
NGC 0063	1160	SDSS/DR8	<i>u, g, r, i, z</i>	6.0	-

Notes. Sample of the table accompanying the data release on the CDS. Only the first ten lines of the file are shown here. Columns 1 and 2 are the galaxy common name and number from the Catalogue of Principal Galaxies (PGC); column 3 is the origin of the image, identifying the data release in the case of the SDSS, and the instrument in the case of the new LT images; columns 4 and 5 are the bands made available and the size of the images (all images are square); and column 6 identifies the calibration method used in the case of the LT images (see Sect. 2.3).

limits in volume, magnitude, and size ($d < 40$ Mpc, $m_B < 15.5$, $D_{25} > 1$ arcmin, as obtained from HyperLEDA), though avoiding the plane of the Milky Way ($|b| > 30^\circ$).

Many of the science themes that can be tackled with S⁴G data (see Sheth et al. 2010 for an overview, and Martín-Navarro et al. 2012 or Elmegreen et al. 2013 for examples) can benefit from, or may even need, additional imaging at optical wavelengths. This can be for various reasons, for instance to compare directly with previous work that will mainly have been done in the optical, to trace different stellar populations, to use mid-IR-optical colour maps or profiles, and/or to explore the effects of dust extinction. In addition, optical data are vital for any analysis of spectral energy distributions in galaxies, which are especially powerful if data at a wider wavelength range can also be incorporated (e.g., from *GALEX*). This is illustrated by our recent study of the edge-on galaxy NGC 7241 and its newly discovered foreground companion (Leaman et al. 2014).

For most of the S⁴G sample galaxies, optical imaging is publicly available from the Sloan Digital Sky Survey (SDSS; York et al. 2002). In this paper, we present re-processed SDSS images in five bands of 1657 S⁴G galaxies, which we make available as easy-to-use FITS files that can be downloaded by any interested researcher. These images cover an area of at least 1.5 times the diameter of a galaxy. We add to this set *g*-band images of an additional 111 S⁴G galaxies which we obtained with the Liverpool Telescope (LT).

In the second part of the current paper, we use the set of newly reduced SDSS images and an extensive database search to identify nearby companions to S⁴G galaxies, as well as those S⁴G galaxies that are either interacting or merging. We provide lists and images of these galaxies and their companions for further scrutiny, and derive fractions of interacting galaxies and those with close companions in the local Universe. As the currently favoured cosmological model describing the early and subsequent evolution of structure in the Universe relies on galaxy-galaxy interactions and mergers to explain the current population of galaxies and its properties, the detailed study of interacting galaxies is of paramount importance. Our catalogue of interacting or merging galaxies and of those with companions provides a new sample for such study, while the fractions of such galaxies in the nearby Universe provide important calibrations for any cosmological model incorporating galaxy-galaxy interactions.

2. Sample selection, observations, and data reduction

2.1. Sample selection

We started out by selecting all those galaxies in the original S⁴G sample (as defined by Sheth et al. 2010) that had imaging in the seventh Data Release (DR7; Abazajian et al. 2009) of the SDSS. This search yielded 1252 galaxies. Later, we added another 183 galaxies for which imaging was released in SDSS DR8 (Aihara et al. 2011) but which were not in DR7, and 222 galaxies from the new extended S⁴G for all but five of which we used DR8 data. The total number of galaxies for which we re-processed and now release SDSS imaging is thus 1657. These galaxies are identified in Table 1.

We also identified those galaxies in the northern hemisphere (defined here as having declination > -10 deg) which were not included in the SDSS imaging survey. This yielded 185 galaxies, of which 10 have diameters D_{25} larger than 8 arcmin. A total of 111 of these galaxies with diameters smaller than 8 arcmin (see Table 1) was observed by us in only the *g*-band, using the LT on La Palma, as described below.

We thus present images in the full set of five SDSS bands (*ugriz*) for 1657 galaxies, and images in the *g'*-band for an additional 111 galaxies. This amounts to optical imaging for 1768 galaxies in total, or two-thirds of the S⁴G sample.

2.2. Sloan Digital Sky Survey imaging

We use imaging from the SDSS DR7 (for 1257 galaxies) and SDSS-III DR8 (for 400 galaxies). No further imaging data has been, or will be, released by SDSS-III since DR8. The SDSS/SDSS-III data are freely available from the corresponding archive servers. We worked with the “corrected frames” produced by the SDSS photometric pipeline, but we carried out our own background subtraction for both datasets. We then produced FITS files of a size which covers at least three times the diameter of the galaxies but with a

minimum size of 5.0 arcmin, with subtracted backgrounds, and with the images in the five bands aligned so they can be downloaded and used easily. We will describe now some of the main aspects of this process, and of the released images.

2.2.1. SDSS DR7 mosaics, calibration and image quality

The SDSS Data Archive Server (DAS) distributes flat-fielded, calibrated images, so-called “corrected” (“fpC”) frames, taken by the SDSS CCD camera (Gunn et al. 1998).³ Each single frame covers 13.51×9.83 arcmin. As we aim to cover a field of at least three times D_{25} , in several cases the mosaics contain two or even more adjacent fields. The sky subtraction was carried out on each single frame prior to the mosaic assembly.

Before estimating the background level, we subtract the 1000 counts of the SOFTBIAS added to all SDSS images. We apply conservative masking of our target object. The mask has a radius of $1.5 \times R_{25}$; for highly inclined objects the mask shape is an ellipse with ellipticity and position angle taken from the HyperLeda Catalog and corresponding to those of the target galaxy. We then measure the fluxes in about ten thousand randomly placed five pixel-wide apertures. We apply a resistant mean to the distribution of the aperture fluxes, and carry out several iterations to mitigate the effect of stars and other background objects. The SDSS background is very smooth: the frame-to-frame variation of the skylevel is usually $\lesssim 0.2$ ADU, provided no large-scale gradient is present. The mean of the bias-free distribution provides a good estimate of the sky background, and is then subtracted from the images. This value is also displayed in the header for every single field contained within the mosaic. After removing the background level, we assemble the final mosaics in all five bands, centred on the target galaxy, by using SWarp (Bertin 2010).

As the DR7 database covers one single epoch for the entire survey area, the depth of the mosaics corresponds to that of one single exposure in SDSS. We did not include the multi-observations of the SDSS Supernova Legacy Survey for any galaxies that might be located in the survey area of Stripe82 (e.g., Bakos & Trujillo 2012). The 95% completeness limits of the images for point sources are 22.0 mag in u' , 22.2 in g' , 22.2 in r' , 21.3 in i' , and 20.5 in z' (Stoughton et al. 2002 [Early Data Release]; Abazajian et al. 2004, 2009 [DR2,DR7]). Because of the exquisite sky background behaviour, the SDSS images can be used to derive surface brightness profiles down to $\mu_r \sim 27$ mag arcsec $^{-2}$ (Pohlen & Trujillo 2006).

The counts in the images are in ADUs. In the header of each image, we provide the magnitude zeropoints (“magzpt”) to convert the number counts F into magnitudes, as $\text{mag} = -2.5 \times \log F + \text{mag}_{\text{zp}}$.

The SDSS DR7 photometric calibration is reliable on a level of 2%. We opted to follow the traditional recipe to determine the zeropoint of the galaxy mosaic by using the aa, kk, and airmass parameters (the photometric zeropoint, the extinction coefficient and the airmass coefficient). These parameters are provided in the tsField table associated with the exposure containing the target object. The magnitude zeropoint can be given as $-2.5 \times (0.4 \times [\text{aa} + \text{kk} \times \text{airmass}] + 2.5 \times \log(t_{\text{exp}}))$, where the exposure time for each pixel equals 53.907456 s. To calibrate in surface brightness, one uses the pixelscale of 0.396 arcsec/pixel and the standard expression $\text{zp}_{\mu} = \text{zp}_{\text{mag}} + 2.5 \times \log(\text{pixelscale}^2)$.

2.2.2. DR8 specific issues

The SDSS-III imaging is available from the SDSS-III Science Archive Server. Starting with DR8, the SDSS data releases distribute flat-fielded, sky-subtracted, and calibrated fields in the form of multi-extension FITS files. The sky subtraction was done by an improved algorithm compared to previous data releases that had generally overestimated the sky level. After masking the brightest sources, the background has been modelled by a spline fit over heavily binned and smoothed data (further details can be found in Blanton et al. 2011). This background model can easily be recovered from the multi-extension FITS files and added back into the images.

To be consistent with the treatment of DR7 imaging, we reproduced the non-sky-subtracted images of the DR8 galaxies. Then, we followed the same steps in creating the mosaics as we did with the DR7 data. Comparison of the DR8 sky level with that derived by us shows that the values agree very well. There is a small systematic offset: our sky values are in the median 0.15% ($\pm 0.2\%$) lower than those of DR8 and we also find a slight dependency on the level of the background itself (the relative difference grows to around 0.3% for the smallest sky values, and is around zero for the largest). The DR8 sky values are thus slightly overestimated compared to what we determined. This difference could be caused by a different sigma-clipping and/or iteration. This relative difference is rather small, but when studying, for instance, the faint outskirts of galaxies, at levels of ~ 27 mag $^{-2}$ in the r' -band, the difference in sky level could become important.

The calibration of SDSS-III imaging is fundamentally different from that in SDSS-I/II. There was no auxiliary photometric telescope (PT) involved, and the SDSS-III calibration is based on an internal calibration called “ubercalibration” (Padmanabhan et al. 2008; Aihara et al. 2009), which basically compares the overlaps between adjacent scans within the survey. This forces DR8 to be on the same zeropoint on average as the DR7 calibration, but it does not use any data from the PT.

Due to this, in SDSS-III the fluxes are expressed in terms of the rather frivolously named “nanomaggies”, not ADUs. In this description, a “maggy” is the flux f of the source relative to the standard source f_0 , which defines the zeropoint of the magnitude scale. Therefore, a “nanomaggy”, or nMgy, is 10^{-9} maggy. To relate these quantities to standard magnitudes, an object with flux F given in nMgy has a Pogson magnitude $m = -2.5 \times \log F + 22.5$.

The standard source for each SDSS band is close to but not exactly the AB source (3631 Jy, Fukugita et al. 1996), meaning that a nanomaggy is approximately 3.631×10^{-6} Jy. However, the absolute calibration of the SDSS system has some percent-level offsets relative to AB. The u band zeropoint is in error by 0.04 mag, in the sense that $u_{\text{AB}} = u_{\text{SDSS}} - 0.04$ mag, while g, r , and i are close to

³ The dark current is negligible, the gain is around 3 e-/ADU, and the readout noise is generally less than or around 5 e-/pixel. The exact values as measured during the observations are reported in the corresponding “tsField” files, although we did not save this specific information in the headers of our mosaics.

AB. The z -band zeropoint is not as certain, and may be shifted by about 0.02 mag in the sense $z_{\text{AB}} = z_{\text{SDSS}} + 0.02$ mag (Abazajian et al. 2004; the same offsets have to be applied to the DR7 imaging as well, when transforming into the AB system.)

2.2.3. Advantages of the re-reduced images

Through this release, the optical imaging for two-thirds of the S⁴G sample galaxies can easily be accessed in FITS format. The naming convention includes the identification of the target galaxy and the filter, for instance, the r' -band mosaic of PGC 01107 is called: PGC01107rmosaic.fits. The sky-subtraction algorithm and the mosaicing were both optimised to cope with the presence of large galaxies. We inspected all images visually, and manually corrected any discrepancies where the automatic pipeline might have failed. The large image size (at least $3 \times D_{25}$ is covered in all filters) is an important aspect which allows one to explore (1) the immediate vicinity of these galaxies, and (2) the faintest structures observable with SDSS imaging, including surface brightness profiles out to $\sim 2 \times R_{25}$. Our images obviously maintain the excellent background and noise characteristics, and excellent photometric and astrometric calibration, of the SDSS image survey. An illustration of these advantages can be seen in Fig. 1.

2.3. Liverpool Telescope imaging

The LT (Steele et al. 2004) is a 2.0 m robotic telescope situated in the Roque de Los Muchachos Observatory on the island of La Palma. We have used two different cameras for our project, namely RATCam and IO:O, to observe a total of 111 S⁴G galaxies which had not been observed in the SDSS, are smaller than 8 arcmin, and at a declination > -10 deg.

RATCam has now been retired from the LT. The field of view (FOV) was 4.6×4.6 arcmin, with a pixel scale of 0.1395 arcsec/pixel. We observed 5 galaxies with RATCam between September and October 2011, using a Sloan g' -band filter. Each galaxy was observed for 3×100 s.

RATCam was replaced by the IO:O camera⁴. It provides a wider field of view and greater sensitivity than RATCam. The FOV is 10×10 arcmin and the pixel scale is approximately 0.15 arcsec/pixel. However, we used the 2×2 binning because the 1×1 binning was not operative at the time of the observations, with a resulting pixel scale of 0.3008 arcsec/pixel. We observed 106 galaxies with IO:O using a Sloan g' -band filter, also with 3×100 s exposure time, in February 2012 and from July 2012 to January 2013.

LT images are delivered after having passed a basic data reduction pipeline, which includes bias subtraction and flat-fielding correction. The overscan regions are trimmed off, leaving a 2048×2048 pixel image. We subtracted the background before, and again after the combination of the three separate exposures by determining the background from regions well outside the galaxy, ignoring emission from, e.g., foreground stars or cosmetic defects by combining with a median algorithm. If one of the three individual exposures had significantly different seeing from the others, it was rejected before the combination. Also, if some of the frames presented strange features (e.g., a satellite track, humidity problems), the corresponding images were rejected. For flux calibration, a set of Landolt standard stars was observed in all the bands every two hours, specifically PG0231+051, RUBIN 149, PG1047+003, PG1525-071A, MARK-A and PG2331-055A. To transform from the $UBVR_{\text{clc}}$ filter set used in the literature to $ugriz$, we used the equations presented in Smith et al. (2002). We computed the corresponding zero-points to perform the photometry, and added them to the headers of the images (stored in keyword COMMENT2). For the nights when no standard stars were observed, we performed the flux calibration by computing the g' magnitude using $BVRI$ photometry values obtained from the NED, as described below.

The headers contain a keyword COMMENT3 with information about the calibration method used. This information is expanded in Table 1, as follows: 1. – standard stars, 2. – cross-calibrated using a total g' magnitude as derived from photometry in NED, from different bands, namely 2.1 – g' computed from B and V , 2.2 – computed from B and R , 2.3 – from B and I , 2.4 – from B , R and I , and 2.5 – from b and J . In all cases we performed linear correlations using predictions based on the MIUSCAT stellar populations models. This set of predictions is an extension of the Vazdekis et al. (2003, 2010) models, based on the Indo-U.S., CaT and MILES empirical stellar libraries. A full description of the models is given in Vazdekis et al. (2012) and applications are provided in Ricciardelli et al. (2012). The equations used are $g' = R + 0.7232(B - R) + 0.0224$, $g' = I + 0.7902(B - I) + 0.0517$ and $g' = J + 0.8413(B - J) + 0.0927$, with a correlation coefficient R^2 of over 99.5%. The LT images of four galaxies have a value X in keywords COMMENT2 and COMMENT3. These images, of UGC 09992, UGC 10194, PGC 027825 and PGC 029086, could not be calibrated because we did not have standard star observations, nor photometric information to calculate a total g' magnitude. In spite of this, we do release the images.

The final images have a seeing between 1 and 3 arcsec, with a median seeing value of 1.4 arcsec. The final list of galaxies for which we present LT g' -band images is shown in Table 1, which also lists other basic parameters of the images such as the instrument and calibration method used.

3. Image quality control

We checked all images by eye, aiming to ensure that all images are properly reduced and consistent. The LT images were checked during the data reduction procedure. As there were relatively few LT images and as they were treated individually, no additional quality control was necessary. For the SDSS images, which constitute the bulk of our images (over 8000 in total), we developed two simple scripts, the first of which identifies images with more than a small number of non-physical pixels, and the second of which displays the images in all five bands for a certain galaxy in one image display window, scaling them logarithmically.

We thus identified a few images with problems, which were corrected by re-processing the data. A small number of galaxies (< 1% of the total) were found to be near the edge of the SDSS survey area. We left these in as the images may still be useful, even if the outer region of a galaxy is not completely visible (e.g., NGC 6118). Finally, when producing the false-colour images we

⁴ <http://telescope.livjm.ac.uk/Info/TelInst/Inst/IOO/>



Fig. 1. False-colour image of the Virgo cluster spiral NGC 4321 (M100).

realised that a small fraction ($\sim 2\%$) of the DR7 images had a different astrometric orientation, $X=N$ and $-Y=E$ instead of $Y=N$ and $-X=E$. For some reason which we do not understand and which we have not seen documented in the literature, galaxies at low latitudes are sometimes given this incorrect astrometric solution. We easily corrected this by applying a rotation-transposition-rotation transformation. An example of this is NGC 1055 (the various SDSS images shown on the ‘images’ page for this galaxy on the NED illustrate the problem). After these checks, all released images should be directly useful for science, although given the large number of them we cannot guarantee the complete absence of small defects.

4. False-colour images

We used the images described above to produce false-colour images of 29 selected galaxies from our sample, which we release publicly for their use in, for instance, scientific presentations and in public outreach work. For this, we selected primarily large galaxies, which will yield images with high resolution across the galaxies and their components, and particularly interesting galaxies, such as interacting and merging galaxies, or with features such as rings, loops, warps, or dust lanes. All attempts were made to produce aesthetically pleasing images that attempt to capture appropriate details and colours approximating true-colour images.

To produce these images, an example of which is shown in Fig. 1 for the galaxy NGC 4321, we scale the different images in such a way as to show their structure in the most clear and aesthetically pleasing way, rather than in an alternative way which would be to scale them approximately and then combine them to produce the equivalent of an “RGB” image with no further cosmetic work. The latter approach may be more reproducible but will lead to ugly images.

The first step in the production of these images is to scale the raw FITS files to show the outer spiral arms as well as the detail in the centre of the galaxy. We start out with three images, usually those in the g , r and i bands, and then include the *Spitzer* $3.6\mu\text{m}$ S⁴G image as obtained from the IRSA archive, and in most cases the SDSS u and z -band images, although the latter do not tend to add significantly to the end result. Aiming to represent typical expected colours such as blue for young stellar populations and red and brown for dust lanes, we use the g -band data as the blue channel, the r -band data for red, and a mixture of u , z and $3.6\mu\text{m}$ added to the i -band data for the green channel in order to produce a balanced equivalent to three-band images and to highlight certain

features that were enhanced by using in particular the *Spitzer* infrared data. This methodology introduces a lot of "false" colour into the images but is ultimately the most successful way to produce images for the use intended here, which is not so much scientific, but primarily for illustrative and public outreach purposes.

The effort in producing the final images comes mainly from the combination of the various images, their scaling, correction of background levels, and cosmetic edits (including colour shifts, cosmetic repair of uneven sky backgrounds, or shifted star colours).

5. Image availability

5.1. Science images

All science images are released publicly with the publication of this paper. They can be used freely by any researcher interested, provided the origin of the images is identified as this paper, SDSS or LT, and the data archive they were downloaded from. Images are available through the NASA-IPAC Extragalactic Database (NED) and the Centre de Données astronomiques de Strasbourg⁵ (CDS) in FITS format. The headers of the images give information on the origin of the image, filter and other instrumental parameters, and calibration information. A README file accompanies the data release on the CDS, listing the galaxies, the images with their sources, the size of the images, and the calibration method used in the case of LT data. The first ten lines of this README file are shown here as Table 1.

The S⁴G images of these galaxies in the 3.6 and 4.5 μm bands are released by the S⁴G team through the IRSA, and do not form part of the data release related to this paper.

5.2. False-colour images

The resulting false-colour images are available publicly from the website of the EU-funded Initial Training Network DAGAL (Detailed Anatomy of GALaxies, www.dagalnetwork.eu), and can be used freely for any purpose provided the origin of the images is clearly acknowledged. We supply the images as jpeg files of various sizes, as well as high-resolution tiff files for use in professional printing applications.

6. Interacting and companion galaxies

We used our visual inspection of all images of over 1700 nearby galaxies with SDSS imaging as the starting point to make an inventory of which of the S⁴G sample galaxies have a close companion, and which are interacting or merging. This allows a direct estimate of the fraction of galaxies in these categories, and defines samples for future study, either of individual galaxies, or of their collective properties, such as for example the star formation rate (which has been found to be enhanced in galaxies with a close companion, see, e.g., Knapen & James 2009 and references therein).

6.1. Close companions

To define which galaxies have a close companion nearby and massive enough to plausibly cause gravitational tidal effects, we follow the approach of Knapen & James (2009), which in turn was based on works by Schmitt (2001), Laine et al. (2002), and Knapen (2005). We consider a galaxy to have a close companion if this companion (1) is within a radius (measured from the centre of the galaxy) of five times the diameter of the sample galaxy, or $r_{\text{comp}} < 5 \times D_{25}$, with D_{25} from the RC3, and (2) has a recession velocity within a range of $\pm 200 \text{ km s}^{-1}$ of the galaxy under consideration, and (3) is not more than 3 mag fainter (using magnitudes in NED). As a rough indication, $5 \times D_{25}$ corresponds to around 50 kpc in most survey galaxies, although in some cases this distance can be as large as 200 kpc (depending on the size of a galaxy and its distance to us). The precise value for each galaxy with a close companion can be derived from Table 3.

To find galaxies that qualify under these criteria, we performed an automated search of all 2829 galaxies in the S⁴G sample (original plus extended) using NED. We then filtered the results to end up with a list of those galaxies that have a close companion, and the name and basic properties of the companion. We went through the list to remove any erroneous entries, such as duplicate galaxies (where NED has the same object listed under different names, with sometimes slightly different positions), or sources within galaxies (e.g., X-ray sources, HII regions).

The list of galaxies with *bona fide* companions is given in Table 3. A total of 470 galaxies of our sample of 2829 galaxies have a companion by the criteria identified above (17%). One can argue whether these criteria are optimal, but we feel that they are a good compromise to find companions which are massive and nearby enough so they can be expected to have a tidal gravitational impact on the sample galaxy. Our second criterion, of relative recession velocities within $\pm 200 \text{ km s}^{-1}$, can be widened, but more unrelated neighbouring galaxies would creep in. However, we do note the case of NGC 3384 and its companion M 105 (NGC 3379) at 7.2 arcmin, 0.6 mag brighter, and $\Delta v = 207 \text{ km s}^{-1}$, where we are most likely dealing with a galaxy pair, but which cannot be formally catalogued here as a close companion. In addition, two galaxies which were catalogued as having a close companion have other companions which fall just outside the criteria (NGC 4106 with companion NGC 4105 at 1 arcmin, 0.76 mag brighter, and $\Delta v = -214 \text{ km s}^{-1}$; and NGC 5560 with companion NGC 5566 at 5.2 arcmin, 1.7 mag brighter, and $\Delta v = -222 \text{ km s}^{-1}$). As we only identified these cases, we estimate that such effects introduce an uncertainty of at most a percent.

It is possible that companions fainter than 3 mag are not catalogued in NED, in particular this is likely to be the case for the faintest of our sample galaxies. We thus calculate the fraction of bright (<13.5 mag, we use this limit because the NED should be

⁵ Via anonymous ftp to cdsarc.u-strasbg.fr (130.79.128.5) or via <http://cdsarc.u-strasbg.fr/viz-bin/qcat?J/A+A/xxx/yyy>

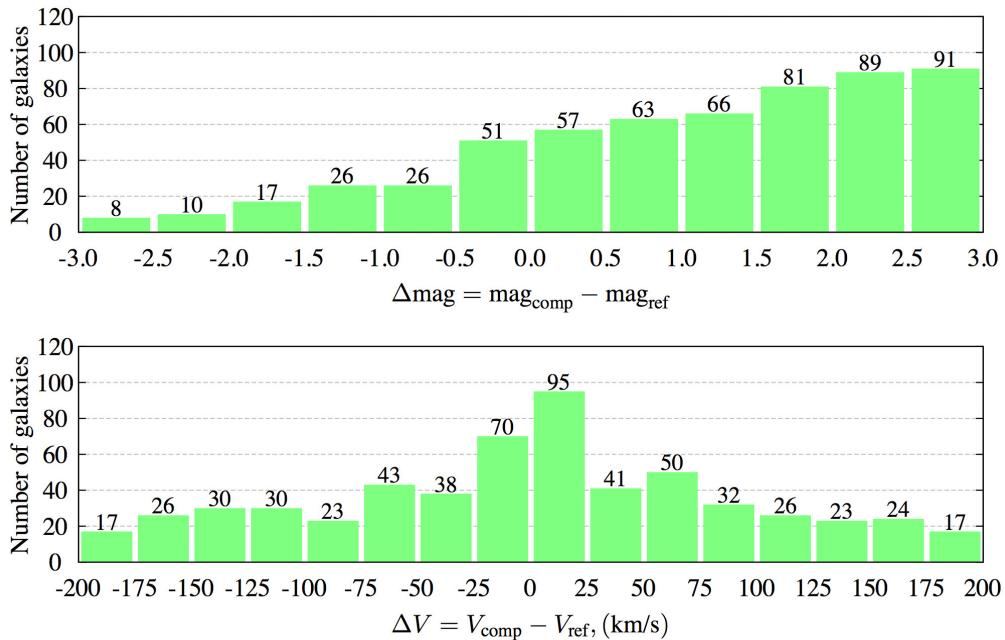


Fig. 2. Histograms showing the distribution of magnitude (top) and recession velocity difference (lower panel) for galaxy-companion pairs.

complete down to 16.5 mag) galaxies with a close companion, which is 21% (267 of 1281 galaxies), and confirm that this is the case. Figure 2 illustrates how the magnitude difference criterion introduces an asymmetry in the results: many more fainter companions are found than brighter ones. For comparison, the lower panel of Fig. 2 shows that the velocity difference between a sample galaxy and its companion is indeed symmetric around 0 km s⁻¹, as expected. Note that we considered every S⁴G sample galaxy separately, and a pair of companions of which both members are in the S⁴G sample will thus be counted twice. Also note that companions which are themselves not S⁴G sample galaxies are included in this plot, so the total number of galaxies included here is larger than the number of S⁴G galaxies with companions.

6.2. Interacting and merging galaxies

In the next step of our analysis, we visually study all galaxies identified to have a close companion in Sect. 6.1, and classify them by the degree of disturbance in appearance related to tidal interactions with the companion. We classify galaxies in three categories for this purpose, plus the remaining and largest category of galaxies which appear undisturbed. The three categories are:

A. Mergers: two similar-size galaxies which are overlapping and very clearly interacting;

B. Highly distorted galaxies, which are interacting as can be judged by morphological hallmarks as tidal arms, or gross distortions of the stellar disk; and

C. Galaxies which show some sign of interaction, such as relatively minor distortions of their disk, or minor tidal features.

As this is based on visual classifications, the criteria are somewhat subjective, but this exercise is nevertheless very efficient to classify galaxies at various stages of interaction and merging. In total, we find 32 (1.1% of the complete S⁴G sample and 7% of the 470 galaxies with close companions) Class-A mergers, 62 (2.2% and 13%) Class-B highly distorted interacting galaxies, and 128 (4.6% and 27%) Class-C interacting galaxies with minor distortions. The remaining galaxies, with a close companion but not in categories A, B, or C, are 248 in total, or 53% of the close companion galaxies. Images for all Class A, B, and C galaxies are shown in Figs. 3, 4 and 5, and these galaxies are identified as such in Table 3.

6.2.1. Comparison with other studies

The Class A, B, and C used here are very similar to the distortion or perturbation indicator (from 0 to 1 on a scale of 5) of the galaxies in the EFIGI catalogue by Baillard et al. (2011), to the categories *M* (merging, roughly our Class A), *T* (tidal, comparable to our B and C) and *N* (non-disturbed) of Lambas et al. (2012), or to the morphological perturbation classes *P* = 0 – 4 as defined by Nazaryan et al. (2014). In fact, Lambas et al. and Nazaryan et al. report similar percentages as we do here, namely 60% for *N*, 30% for *T* and 10% for *M* (Lambas et al. 2012), and 45%, 23%, 22% and 10% for classes *P* 0 to 3, respectively (Nazaryan et al. 2014), corresponding to our measured fractions of 53%, 27%, 13%, and 7% (see previous subsection) for galaxies with a close companion but without signs of interaction, and Class C, B, and A, respectively. The differences can easily be explained by the quite different selection criteria to select close pairs. In particular the fraction of merging galaxies is stable at around 10% among pairs of galaxies in the three studies compared. Other studies using sometimes very different methods yield very similar percentages (e.g., Patton et al. 1997, Darg et al. 2009, Holwerda et al. 2011).

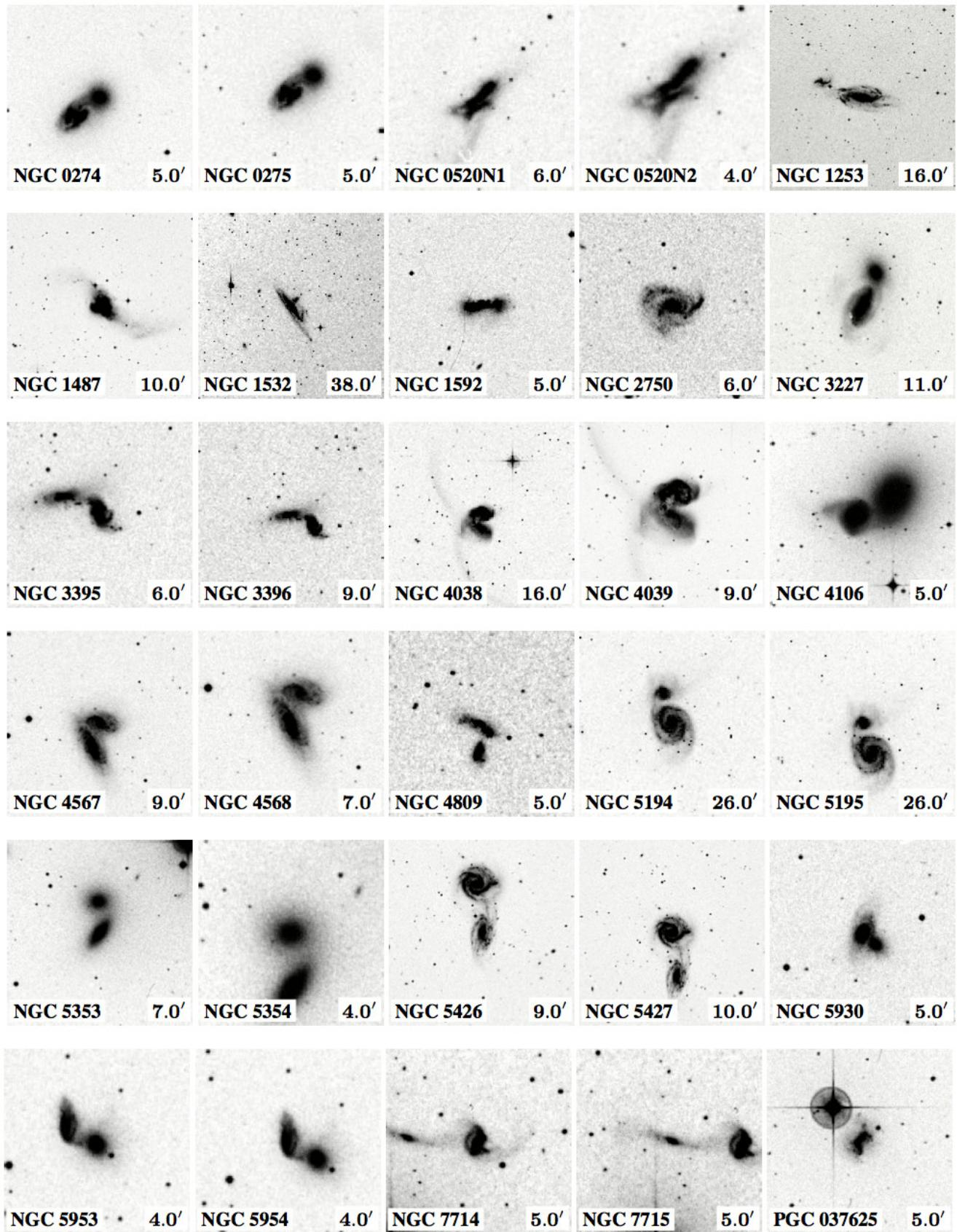
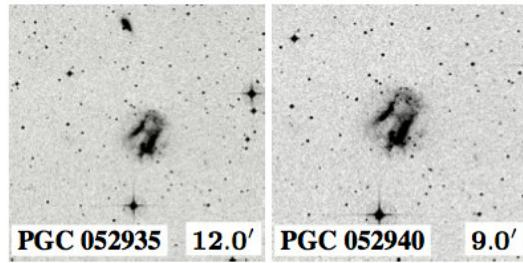


Fig. 3. Class A galaxies, similar-size galaxies which are overlapping and very clearly interacting. Details of the S⁴G sample galaxies and the companions are in Table 3. Images are centred on the galaxy which is identified in the bottom-left label, while the bottom-right label indicates the size, in minutes of arc, of the image shown.

**Fig. 3.** Continued.

We have explicitly considered the overlap in samples between the EFIGI catalogue and ours, to see how well the perturbation indicator of Bailard et al. (2011) correlates with our interaction classes. There are 199 galaxies in common with those of our galaxies which have a close companion (8 in class A, 27 in class B, 47 in class C, and 117 without interaction class). The results of the comparison show that, considering the differences in approach, definitions and data quality, these studies are compatible (the mean perturbation index of our Class A galaxies is 0.67 ± 0.07 , for B 0.62 ± 0.05 , C 0.34 ± 0.04 , and for our remaining galaxies 0.13 ± 0.02).

The S⁴G team have recently performed a complimentary study by carefully studying the very outskirts of the S⁴G galaxies (original sample only) to catalogue any deviations from symmetry at the lowest light levels (Laine et al. 2014). Among other characteristics such as warps, rings, and asymmetries, Laine et al. catalogue from inspection by eye those galaxies with morphological evidence of interactions and past or ongoing mergers. In this, Laine et al. limit themselves to companions visible in the S⁴G image, use a permitted velocity range of 600 km s^{-1} between sample galaxy and companion, and do not reject all cases where a velocity confirmation cannot be found. Even though the approaches are very different, we find a satisfactory degree of complimentarity, with 64% of the galaxies found to have a companion in Laine et al. being classified as having one in the current paper, and 69% for the interacting galaxies.

These various comparisons with other works in the literature show that an analysis such as the one presented here gives valid and reproducible overall results.

6.2.2. Interacting fraction among bright galaxies

We observe that the fraction of interacting galaxies among the PGC, IC, ESO and UGC galaxies in the S⁴G sample is much lower than among the NGC galaxies. The median magnitudes of NGC, IC, ESO, UGC, and PGC galaxies are 12.81, 14.00, 14.66, 14.89, and 14.79, respectively. As the NGC galaxies are brighter and we noted before the possible incompleteness of faint companions to faint sample galaxies, we consider the fraction of interacting galaxies among the NGC sub-sample as a more accurate estimate for the nearby Universe. We thus find that 350 ± 16 of the 1472 NGC galaxies in the S⁴G sample have a close companion, or $23.7\% \pm 1.1\%$ (where all uncertainties quoted are Poisson errors, cf. Laine et al. 2002). 29 (2.0%) are Class A galaxies, 42 (2.9%) are Class B, and 85 (5.8%) are Class C.

Adding Class A and B NGC galaxies leads to an estimate of the fraction of significantly interacting galaxies among the bright part of the local galaxy populations of 71 ± 8 galaxies, or $4.8\% \pm 0.5\%$. This is consistent with previous determinations, such as the number of interacting galaxies of around 4% of bright local galaxies reported on the basis of a much smaller sample by Knapen & James (2009).

6.3. Non-interacting very close companions

We have identified an interesting class of galaxies, namely those with very close companions (closer than 1.5 times the diameter of the sample galaxy) but for which we cannot see any indication of distorted morphology. These 38 galaxies are shown in Fig. 6 and listed in Table 2. Most of these galaxies are of early morphological type, with only five spirals later than type Sb, and only one irregular galaxy (UGC 1176). We thus postulate that most of the galaxies in this category have rather stable, gas-poor disks, which are less susceptible to be distorted by gravitational interactions. They do constitute a curious class of galaxies that warrants further study.

7. Conclusions

We have collected and re-reduced optical images of 1768 of the 2829 galaxies in the sample of the S⁴G survey, which we make available to the community as ready-to-use FITS files to be used in conjunction with the mid-IR images. Of these, 1657 were observed as part of the SDSS. We collected and re-processed images in five bands for these galaxies, producing mosaics which cover an area of at least 5 arcmin or three times the diameter of the galaxy, whichever is largest.

In addition, we observed in the *g*-band an additional 111 S⁴G galaxies in the northern hemisphere with the 2.0 m LT, so that optical imaging is released for 1768 galaxies, or for 63% of the S⁴G sample. We also produce false-colour images of some of these galaxies to be used for illustrative and public outreach purposes.

Table 2. Galaxies with a very close companion but without any sign of interaction.

Galaxy	D_{25} (')	Separation (D_{25})	Type
ESO 467-051	2.8	1.0	SBdm sp
IC 1459	4.6	1.4	E5(s)
IC 1727	6.5	1.2	SB(s)m
IC 2058	3.4	0.5	SB(s)m sp
IC 3313	1.3	0.8	E0(s)
NGC 1199	2.8	1.2	E3(s)
NGC 1596	3.9	0.8	S0 ⁻ sp
NGC 2543	2.2	1.5	SA_B(s)b
NGC 2634	1.7	1.1	S0(s)
NGC 2778	1.3	1.4	E3(s)
NGC 2853	1.7	1.3	E5(s)
NGC 3471	1.7	1.4	SB(s)0a
NGC 3636	2.5	1.5	S0(s)
NGC 3637	2.5	1.5	SB_a0 ⁺
NGC 4216	7.8	1.5	SAB_a
NGC 4309	1.9	0.8	SAB0 ^o
NGC 4417	3.1	0.2	S0(s)
NGC 4486	7.1	1.2	E0(s)
NGC 4666	5.0	1.5	SB(s)c sp
NGC 4961	1.1	1.3	SB(rs) bc
NGC 5403	2.8	0.6	Sab
NGC 5485	2.5	1.5	E0(s)
NGC 5576	2.8	1.0	SA0/a or E3
NGC 5636	1.4	1.4	SAB(r)0/a
NGC 5638	1.9	1.0	
NGC 5775	3.7	1.2	Sc sp
NGC 5777	3.0	0.9	SB0 ⁺
NGC 6255	3.1	0.4	SB(s) d
NGC 6278	1.7	1.4	SA(r)0 ^o
NGC 6868	3.6	0.4	E3(s)
NGC 7173	1.9	0.7	E0(s)
NGC 7176	1.1	0.4	S0(s)
NGC 7187	1.1	0.1	S0a(r)
PGC 045084	2.3	1.4	SB(s)a
PGC 046261	2.5	0.7	Scd sp
UGC 01176	3.9	1.5	Ia
UGC 10043	2.2	1.2	S0/a
UGC 10806	2.1	0.4	SB(s)m

Notes. Properties of galaxies with a companion closer than $1.5 D_{25}$, but in which no signs of interaction are seen in our images. Morphological type from the RC3. Properties of the companion galaxies are in Table 3.

We note from these images and from a NED database search which of the S⁴G sample galaxies have close companions or are interacting, confirming this by determining the radial velocities, projected distances and magnitudes of the galaxies. We find that 17% of the S⁴G galaxies (21% of those brighter than 13.5 mag) have a close companion (within a radius of five times the diameter of the sample galaxy, a recession velocity within $\pm 200 \text{ km s}^{-1}$ and not more than 3 mag fainter), and that around 5% of the bright part of the S⁴G sample show significant morphological evidence of interaction. This confirms and further supports previous estimates of these fractions.

The images described in this paper, the re-processed SDSS ones, the new LLT images, and the false-colour pictures, are publicly released for general use for scientific, illustrative, or public outreach purposes. The galaxies with close companions and, in particular, the interacting galaxies we identified are candidates for further study, either collectively or as case studies.

Acknowledgements. We thank Sébastien Comerón, Benne Holwerda, and an anonymous referee for valuable comments on an earlier version of this paper, and Seppo Laine for discussions. We thank the entire S⁴G team for conceiving, implementing and executing the S⁴G survey. JHK, MC and RL acknowledge financial support to the DAGAL network from the People Programme (Marie Curie Actions) of the European Union's Seventh Framework Programme FP7/2007-2013/ under REA grant agreement number PITN-GA-2011-289313. JR acknowledges the receipt of a summer studentship at the Instituto de Astrofísica de Canarias. JHK, SE-F, JR, JB, MC and RL thank co-author NS for his dedication, time, and effort in collaborating with us in turning FITS images into inspiring and colourful pictures of galaxies—this constitutes another successful Pro-Am collaboration. The Liverpool Telescope is operated on the island of La Palma by Liverpool John Moores University in the Spanish Observatorio del Roque de los Muchachos of the Instituto de Astrofísica de Canarias with financial support from the UK Science and Technology Facilities Council. Funding for SDSS-III has been provided by the Alfred P. Sloan Foundation, the Participating Institutions, the National Science Foundation and the US Department of Energy Office of Science. The SDSS-III web site is <http://www.sdss3.org/>. SDSS-III is managed by the Astrophysical Research Consortium for the Participating Institutions of the SDSS-III Collaboration including the University of Arizona, the Brazilian Participation Group, Brookhaven National Laboratory,

University of Cambridge, Carnegie Mellon University, University of Florida, the French Participation Group, the German Participation Group, Harvard University, the Instituto de Astrofísica de Canarias, the Michigan State/Notre Dame/JINA Participation Group, Johns Hopkins University, Lawrence Berkeley National Laboratory, Max Planck Institute for Astrophysics, Max Planck Institute for Extraterrestrial Physics, New Mexico State University, New York University, Ohio State University, Pennsylvania State University, University of Portsmouth, Princeton University, the Spanish Participation Group, University of Tokyo, University of Utah, Vanderbilt University, University of Virginia, University of Washington and Yale University. This research has made use of NASA's Astrophysics Data System. We acknowledge the usage of the HyperLeda data base and the NASA/IPAC Extragalactic Data base (NED), operated by the Jet Propulsion Laboratory, California Institute of Technology, under contract with the National Aeronautics and Space Administration. We have used data products made available through the Galaxy Zoo collaboration (www.galaxyzoo.org). The Digitized Sky Survey was produced at the Space Telescope Science Institute under US Government grant NAG W-2166.

References

- Abazajian, K., Adelman-McCarthy, J. K., Agüeros, M. A., et al. 2004, AJ, 128, 502
 Abazajian, K. N., Adelman-McCarthy, J. K., Agüeros, M. A., et al. 2009, ApJS, 182, 543
 Aihara, H., Allende Prieto, C., An, D., et al. 2011, ApJS, 193, 29 (Erratum 2011, ApJS, 195, 26)
 Baillard, A., Bertin, E., de Lapparent, V., et al. 2011, A&A, 532, A74
 Bakos, J., & Trujillo, I. 2012, submitted to ApJ (arXiv:1204.3082)
 Bertin, E. 2010, Astrophysics Source Code Library, 10068
 Blanton, M. R., Kazin, E., Muna, D., Weaver, B. A., & Price-Whelan, A. 2011, AJ, 142, 31
 Darg, D. W., Kaviraj, S., Lintott, C. J., et al. 2011, MNRAS, 416, 1745
 Eisenstein, D. J., Weinberg, D. H., Agol, E., et al. 2011, AJ, 142, 72
 Elmegreen, D. M., Elmegreen, B. G., Erroz-Ferrer, S., et al. 2014, ApJ, 780, 32
 Eskew, M., Zaritsky, D., & Meidt, S. 2012, AJ, 143, 139
 Fazio, G. G., Hora, J. L., Allen, L. E., et al. 2004, ApJS, 154, 10
 Fukugita, M., Ichikawa, T., Gunn, J. E., et al. 1996, AJ, 111, 1748
 Gunn, J. E., Carr, M., Rockosi, C., et al. 1998, AJ, 116, 3040
 Holwerda, B. W., Pirzkal, N., de Blok, W. J. G., & van Driel, W. 2011, MNRAS, 416, 2447
 Knapen, J. H. 2005, A&A, 429, 141
 Knapen, J. H., & James, P. A. 2009, ApJ, 698, 1437
 Laine, S., Shlosman, I., Knapen, J. H., & Peletier, R. F. 2002, ApJ, 567, 97
 Laine, S., et al. 2014, submitted to MNRAS
 Lambas, D. G., Alonso, S., Mesa, V., & O'Mill, A. L. 2012, A&A, 539, A45
 Leaman, R., Erroz-Ferrer, S., Cisternas, M., & Knapen, J. H. 2014, submitted to MNRAS
 Martín-Navarro, I., Bakos, J., Trujillo, I., et al. 2012, MNRAS, 427, 1102
 Meidt, S. E., Schinnerer, E., Knapen, J. H., et al. 2012, ApJ, 744, 17
 Meidt, S. E., Schinnerer, E., van de Ven, G., et al. 2014, arXiv:1402.5210
 Nazaryan, T. A., Petrosian, A. R., Hakobyan, A. A., McLean, B. J., & Kunth, D. 2014, Astrophysics, 57, 14
 Padmanabhan, N., Schlegel, D. J., Finkbeiner, D. P., et al. 2008, ApJ, 674, 1217
 Patton, D. R., Pritchett, C. J., Yee, H. K. C., Ellingson, E., & Carlberg, R. G. 1997, ApJ, 475, 29
 Pohlen, M., & Trujillo, I. 2006, A&A, 454, 759
 Ricciardelli, E., Vazdekis, A., Cenarro, A. J., & Falcón-Barroso, J. 2012, MNRAS, 424, 172
 Schmitt, H. R. 2001, AJ, 122, 2243
 Sheth, K., Regan, M., Hinz, J. L., et al. 2010, PASP, 122, 1397
 Smith, J. A., Tucker, D. L., Kent, S., et al. 2002, AJ, 123, 2121
 Steele, I. A., Smith, R. J., Rees, P. C., et al. 2004, Proc. SPIE, 5489, 679
 Stoughton, C., Lupton, R. H., Bernardi, M., et al. 2002, AJ, 123, 485
 Vazdekis, A., Cenarro, A. J., Gorgas, J., Cardiel, N., & Peletier, R. F. 2003, MNRAS, 340, 1317
 Vazdekis, A., Sánchez-Blázquez, P., Falcón-Barroso, J., et al. 2010, MNRAS, 404, 1639
 Vazdekis, A., Ricciardelli, E., Cenarro, A. J., et al. 2012, MNRAS, 424, 157
 York, D. G., Adelman, J., Anderson, J. E., Jr., et al. 2000, AJ, 120, 1579

Table 3. Properties of galaxies with close companions, and of interacting galaxies.

Galaxy	Inter.	D_{25} (')	Vel. (km/s)	mag.	Separation (')		Optical
					D_{25}	(kpc)	
ESO 027-001		2.7	2570	12.2	7.9	2.9	78.4
ESO 027- G 003			2578	14.8			
ESO 079-003		3.0	2616	12.6	8.2	2.7	87.4
ESO 079- G 002			2756	13.7			
ESO 185-027		1.4	2167	13.8	4.2	3.1	34.5
6dF J1956175-565025			2112	16.3			
ESO 236-039	B	1.0	1574	15.1	3.1	3.1	18.4
AM 2141-491 NED01 SE			1546	15.6			
AM 2141-491 NED01 NW			1586	15.2			
ESO 249-035		1.6	1031	16.2	3.4	2.1	11.8
Horologium Dwarf			898	15.1			
ESO 249-036		1.2	898	15.1	3.4	2.8	13.6
ESO 249- G 035			1031	16.2			
ESO 293-034	C	2.5	1512	13.7	1.1	0.4	6.1
MCG -07-01-010			1428	14.6			
ESO 342-013	B	1.6	2614	13.8			

Table 3. Continued.

Galaxy	Inter.	D_{25} (')	Vel. (km/s)	mag.	Separation (')	D_{25}	Optical (kpc)
APMUKS(BJ) B210710.73-374124.			2623	16.1	3.9	2.4	39.7
ESO 356-018		1.7	1438	15.5			
6dF J0255394-362008			1515	15.8	5.8	3.4	34.1
ESO 361-019	B	1.5	2324	14.2			
2MASX J04550020-3715351			2292	15.8	3.9	2.6	34.9
ESO 400-026	B	1.4	2386	15.1			
ESO 400- G 027			2402	15.2	2.9	2.1	27.3
ESO 402-025	C	1.0	2571	16.4			
ESO 402- G 026			2708	13.7	4.5	4.5	47.1
ESO 402-026	C	3.0	2708	13.7			
ESO 402- G 025			2571	16.4	4.5	1.5	44.7
ESO 411-013		1.2	1760	15.8			
ESO 411- G 012			1703	15.7	4.0	3.3	26.4
ESO 441-017	C	2.1	2117	13.7			
6dF J1211186-311431			2135	16.1	7.3	3.5	60.0
ESO 467-051		2.8	1808	14.8			
NGC 7259			1782	13.9	2.9	1.0	19.9
ESO 481-018	C	2.9	1796	13.5			
2MASX J03184089-2545279			1679	16.4	5.0	1.7	32.6
ESO 505-008	C	1.4	1921	15.3			
ESO 505- G 007			1776	17.5	5.9	4.2	40.2
ESO 509-074		2.8	2581	14.0			
6dF J1336008-235518			2611	15.9	10.1	3.6	102.5
ESO 510-058	B	1.2	2337	13.3			
UGCA 383			2337	13.6	2.1	1.7	18.7
ESO 510-059	B	2.3	2337	13.6			
UGCA 382			2337	13.3	2.1	0.9	18.7
ESO 532-014	C	1.6	1719	15.2			
ESO 532- G 015			1746	15.8	5.3	3.3	35.8
ESO 532-022	B	1.5	2603	14.8			
AM 2206-272 NED01			2593	14.6	4.8	3.2	48.2
ESO 576-040	C	2.2	2080	14.9			
[CCF97] G8			2080	16.9	1.4	0.6	11.1
ESO 580-034	C	1.4	2796	15.5			
NGC 5757			2677	13.5	3.6	2.6	37.6
ESO 581-025	C	3.2	2268	13.5			DR8
2MASX J15133820-2045293			2230	14.6	5.3	1.6	45.4
IC 0167	C	1.6	2931	13.6			DR8
NGC 0694			2950	14.3	5.6	3.5	63.8
IC 0223	C	1.1	1579	14.1			
NGC 0899			1563	12.9	5.0	4.5	30.2
IC 0630		3.2	2182	13.5			LT
MRK 1258			2041	15.0	11.3	3.5	89.5
IC 0749	C	2.1	807	13.4			SDSS
IC 0750			701	12.8	3.4	1.6	9.2
IC 0750	B	2.1	701	12.8			SDSS
IC 0749			807	13.4	3.4	1.6	10.6
IC 0755	C	1.5	1524	14.0			SDSS
MRK 0756			1478	14.7	5.9	3.9	33.7
IC 0764	C	4.9	2132	12.8			
ESO 441- G 014			2146	15.0	20.5	4.2	170.0
IC 1048		2.1	1636	13.6			SDSS
UGC 09485			1706	14.9	7.5	3.6	49.6
IC 1066	C	1.2	1577	13.9			SDSS
IC 1067			1577	13.5	2.2	1.9	13.6
IC 1067	C	1.8	1577	13.5			SDSS
IC 1066			1577	13.9	2.2	1.2	13.6
IC 1459		4.6	1802	11.0			DR8
IC 5264			1940	13.7	6.5	1.4	49.1
IC 5269B			1667	13.2	14.5	3.2	93.2

Table 3. Continued.

Galaxy	Inter.	D_{25} (')	Vel. (km/s)	mag.	Separation (D_{25})		Optical
				(\prime)	(\prime)	(kpc)	
IC 1727		6.5	345	12.1			DR8
NGC 0672			429	11.5	8.1	1.2	13.4
IC 2039		1.1	817	14.9			DR8
IC 2038			712	14.9	1.8	1.6	4.9
IC 2058		3.4	1379	13.9			
2MASX J04180709-5555503			1369	16.2	1.8	0.5	9.5
IC 2085		2.5	982	13.9			
NGC 1617			1063	11.4	11.3	4.5	46.6
IC 3059		1.7	258	14.7			SDSS
IC 3066			375	15.6	5.3	3.1	7.7
IC 3155		1.0	2292	14.4			SDSS
VCC 0388			2124	17.4	4.5	4.5	37.2
IC 3259		1.6	1406	14.2			SDSS
VCC 0711			1496	16.8	6.3	4.0	36.6
IC 3313		1.3	1073	15.0			DR8
LSBC F644-04			1087	15.9	1.1	0.8	4.6
IC 3474		2.2	1727	14.8			SDSS
VCC 1459			1774	16.3	4.2	1.9	28.6
IC 3522	C	1.1	668	15.8			SDSS
VCC 1574			639	17.3	4.1	3.7	10.0
IC 4468	C	2.3	2447	13.8			
ESO 580- G 005			2376	15.5	3.6	1.6	33.2
IC 4943		1.3	2969	13.6			DR8
NGC 6861B			2953	15.1	7.0	5.3	80.3
IC 5007	C	2.3	2720	12.6			
IC 5003			2702	13.2	10.0	4.3	104.4
IC 5013	C	3.0	2325	12.7			DR8
ESO 400- G 030			2342	13.5	1.0	0.3	9.0
ESO 400- G 027			2402	15.2	11.1	3.7	102.7
IC 5039		2.3	2702	13.2			
IC 5007			2720	12.6	10.0	4.3	105.1
IC 5264		2.5	1940	13.7			
IC 1459			1802	11.0	6.5	2.6	45.6
2MASX J22571092-3640103			1945	15.8	7.8	3.1	58.6
IC 5267	C	5.6	1712	11.4			
IC 5267B			1737	12.7	22.0	3.9	148.1
IC 5269B		3.5	1667	13.2			
IC 1459			1802	11.0	14.5	4.1	100.7
NGC 0134	B	8.3	1582	11.4			
NGC 0131			1410	13.8	9.1	1.1	49.8
NGC 0210		5.0	1636	12.5			
MCG -02-02-083			1621	14.9	21.6	4.3	135.4
NGC 0216		1.3	1544	12.9			SDSS
ESO 540- G 014			1654	15.4	6.3	4.8	40.3
NGC 0254		2.8	1629	12.6			
6dF J0046510-313227			1510	15.3	10.6	3.8	61.8
NGC 0274⁶	A	1.3	1750	12.8			DR8
NGC 0275			1744	13.2	0.8	0.6	5.5
NGC 0275⁶	A	1.7	1744	13.2			DR8
NGC 0274			1750	12.8	0.8	0.5	5.6
NGC 0470	C	2.9	2374	12.5			DR8
NGC 0474			2325	12.4	5.5	1.9	49.1
NGC 0474	C	2.6	2325	12.4			DR8
NGC 0470			2374	12.5	5.5	2.1	50.1
NGC 0520 NED02⁷	A	4.1	2206	13.6			
NGC 0520 NED01			2266	12.4	0.2	0.1	1.8
UM 102			2188	16.5	4.2	1.0	35.1

⁶ Arp 140⁷ Arp 157

Table 3. Continued.

Galaxy	Inter.	D_{25} (')	Vel. (km/s)	mag.	Separation			Optical
					(')	D_{25}	(kpc)	
MCG +00-04-124			2240	16.0	13.6	3.3	117.5	
NGC 0520 NED01 ⁷	A	4.1	2266	12.4				
NGC 0520 NED02			2206	13.6	0.2	0.0	1.5	
NGC 0524		3.4	2379	11.3				DR8
NGC 0516			2451	14.1	9.8	2.9	92.9	
NGC 0584	C	3.8	1802	11.4				DR8
NGC 0586			1875	14.3	4.3	1.1	31.1	
NGC 0660	B	4.6	850	12.0				SDSS
IC 0148			774	13.9	21.7	4.7	64.9	
NGC 0672	C	6.9	429	11.5				LT
IC 1727			345	12.1	8.1	1.2	10.8	
NGC 0678	B	3.1	2835	13.3				DR8
NGC 0680			2800	12.9	5.4	1.8	58.9	
IC 1730			2959	15.5	7.7	2.5	88.3	
NGC 0680	C	1.8	2800	12.9				DR8
IC 1730			2959	15.5	3.5	1.9	40.0	
NGC 0678			2835	13.3	5.4	3.0	59.6	
NGC 0681		2.5	1760	12.9				SDSS
MCG -02-05-051			1588	15.2	10.4	4.2	63.8	
NGC 0772	B	4.6	2472	11.1				DR8
NGC 0770			2458	13.9	3.5	0.8	33.0	
NGC 0899	B	1.5	1563	12.9				
IC 0223			1579	14.1	5.0	3.3	30.5	
NGC 0908	C	6.3	1509	10.8				
NGC 0899			1563	12.9	29.7	4.7	179.8	
NGC 0907			1655	12.9	31.3	5.0	200.4	
NGC 0936		4.5	1430	11.1				SDSS
NGC 0941			1608	13.4	12.6	2.8	78.3	
NGC 1042	C	3.9	1371	11.5				SDSS
NGC 1052			1510	12.1	14.7	3.8	85.8	
NGC 1047			1340	14.3	17.3	4.4	89.6	
NGC 1052		3.0	1510	12.1				SDSS
[VC 94] 023858-0820.4			1412	13.5	9.3	3.1	50.7	
NGC 1047			1340	14.3	10.2	3.4	53.0	
NGC 1042			1371	11.5	14.7	4.9	77.9	
NGC 1055	C	6.9	994	11.4				SDSS
MESSIER 077			1137	9.6	30.7	4.4	135.0	
NGC 1068		6.2	1137	9.6				SDSS
NGC 1055			994	11.4	30.7	5.0	118.0	
NGC 1110	C	2.4	1333	14.5				SDSS
SDSS J024839.95-074848.3			1465	17.2	7.5	3.1	42.3	
NGC 1199		2.8	2570	12.4				DR8
NGC 1189			2544	15.2	3.4	1.2	33.6	
NGC 1190			2618	15.2	4.2	1.5	42.1	
NGC 1188			2617	14.8	7.8	2.8	79.0	
NGC 1248	C	1.2	2220	13.7				DR8
MRK 0604			2161	15.5	2.6	2.2	22.1	
NGC 1253 ⁸	A	4.6	1713	12.3				LT
NGC 1253A			1826	14.9	3.8	0.8	26.9	
NGC 1300	C	6.2	1577	11.4				
NGC 1297			1586	12.8	19.7	3.2	121.0	
NGC 1316	C	13.5	1760	9.4				DR8
NGC 1317			1941	11.9	6.3	0.5	47.2	
NGC 1316C		1.5	1800	14.3				
FCC 035			1800	15.3	5.1	3.4	35.2	
NGC 1325		4.3	1591	12.5				
NGC 1315			1615	13.9	21.0	4.9	131.0	
NGC 1332		5.4	1524	12.1				

⁸ Arp 279

Table 3. Continued.

Galaxy	Inter.	D_{25} (')	Vel. (km/s)	mag.	Separation		Optical
					(')	D_{25}	
ESO 548- G 021				1668	14.9	19.3	3.6 124.3
NGC 1325A				1333	13.3	20.7	3.8 106.5
NGC 1359	B	1.4		1973	13.3		
ESO 548- G 043				1931	15.6	6.7	4.8 49.9
NGC 1373		1.2		1334	14.1		DR8
NGC 1374				1294	12.0	4.9	4.0 24.3
NGC 1374		2.9		1294	12.0		DR8
NGC 1373				1334	14.1	4.9	1.7 25.0
NGC 1379		2.7		1324	11.8		DR8
NGC 1387				1302	12.0	11.5	4.3 57.9
NGC 1380		4.6		1877	10.9		DR8
NGC 1380B				1740	12.9	15.6	3.4 105.1
NGC 1381				1724	12.4	19.2	4.2 127.7
NGC 1381		2.6		1724	12.4		DR8
MCG -06-09-008				1693	14.8	6.6	2.6 43.4
NGC 1380B				1740	12.9	9.7	3.8 65.2
NGC 1386		3.4		868	12.1		
NGC 1389				921	13.2	16.1	4.7 56.9
NGC 1387		3.0		1302	12.0		DR8
NGC 1379				1324	11.8	11.5	3.8 58.9
NGC 1399		8.5		1425	10.6		DR8
NGC 1387				1302	12.0	19.0	2.2 95.8
NGC 1379				1324	11.8	29.6	3.5 151.3
NGC 1404		5.0		1947	11.0		DR8
NGC 1427A				2028	13.4	15.8	3.2 124.1
NGC 1412		1.1		1790	13.8		DR8
ESO 482- G 032				1724	15.2	5.3	4.9 35.2
NGC 1414		1.7		1697	14.6		
NGC 1422				1637	14.5	8.1	4.8 51.5
NGC 1415		3.6		1585	12.8		
ESO 482- G 031				1683	15.0	6.3	1.7 40.9
ESO 548- G 070				1422	15.6	17.0	4.7 93.7
NGC 1422		2.5		1637	14.5		
NGC 1414				1697	14.6	8.1	3.3 53.3
NGC 1437B		2.9		1497	14.0		
LSBG F359-072				1546	16.7	14.3	4.9 85.2
NGC 1482	C	2.5		1916	13.1		
NGC 1481				1807	14.8	5.1	2.0 35.6
ESO 549- G 035				1778	15.5	9.2	3.7 63.5
NGC 1487⁹	A	2.7		818	11.9		
NGC 1487 NED02				881	12.3	0.2	0.1 0.7
NGC 1493		3.5		1053	11.8		
ESO 249- G 032				1168	14.7	9.6	2.8 43.5
NGC 1510	C	1.3		913	13.5		
NGC 1512				898	11.1	5.0	3.8 17.3
NGC 1511	C	3.6		1341	11.9		
NGC 1511A				1339	14.2	11.1	3.1 57.4
NGC 1512	C	6.8		898	11.1		
NGC 1510				913	13.5	5.0	0.7 17.6
NGC 1531¹⁰	C	1.5		1169	12.9		DR8
NGC 1532				1040	10.7	1.8	1.2 7.1
NGC 1532¹⁰	A	11.2		1040	10.7		
NGC 1531				1169	12.9	1.8	0.2 7.9
NGC 1549		5.1		1256	10.7		DR8
NGC 1553				1080	10.3	11.8	2.3 49.4
NGC 1553		6.2		1080	10.3		
NGC 1549				1256	10.7	11.8	1.9 57.4

⁹ Pair AM 0354-423¹⁰ Pair AM 0410-325

Table 3. Continued.

Galaxy	Inter.	D_{25} (')	Vel. (km/s)	mag.	Separation (')	D_{25}	Optical
						(kpc)	
NGC 1592	A	1.0	944	14.4			
ESO 421-IG 002 NED01			948	15.3	0.4	0.4	1.5
NGC 1596		3.9	1510	12.1			
NGC 1602			1568	13.3	3.0	0.8	18.2
NGC 1602	C	1.9	1568	13.3			
NGC 1596			1510	12.1	3.0	1.6	17.6
NGC 2460		1.8	1442	12.7			LT
IC 2209			1371	14.3	5.4	3.0	28.8
NGC 2543		2.2	2471	13.2			SDSS
2MASX J08125835+3611542			2483	16.1	3.4	1.5	32.5
NGC 2604A	B	1.5	2078	13.0			SDSS
NGC 2604B			2104	15.6	3.6	2.4	29.3
NGC 2633	C	2.2	2160	12.9			
NGC 2634			2258	12.9	8.0	3.6	70.1
NGC 2634A			2086	14.4	9.8	4.5	79.4
NGC 2634		1.7	2258	12.9			DR8
NGC 2634A			2086	14.4	1.9	1.1	15.3
NGC 2633			2160	12.9	8.0	4.7	67.1
NGC 2634A		1.2	2086	14.4			
NGC 2634			2258	12.9	1.9	1.6	16.5
NGC 2648	C	3.1	2060	12.6			SDSS
CGCG 060-036			2115	15.0	2.4	0.8	19.4
NGC 2679		1.9	2050	13.6			DR8
KUG 0848+311			2046	16.3	6.1	3.3	48.6
NGC 2732		1.8	1960	12.9			
UGC 04832			1957	15.0	4.1	2.3	31.3
NGC 2735	B	1.4	2450	14.1			SDSS
SDSS J090253.00+255612.5			2503	17.0	3.2	2.3	31.3
NGC 2750 ¹¹	A	2.0	2674	12.3			SDSS
MCG +04-22-012 NED01			2669	12.7	0.8	0.4	8.3
NGC 2778		1.3	2049	13.3			DR8
NGC 2779			2105	15.5	1.8	1.4	14.4
NGC 2798	B	2.5	1726	13.0			SDSS
NGC 2799			1673	14.3	1.6	0.6	10.1
UGC 04904			1670	15.0	5.3	2.1	34.4
NGC 2799	B	1.8	1673	14.3			SDSS
NGC 2798			1726	13.0	1.6	0.9	10.5
SDSS J091722.70+415953.9			1812	15.1	1.6	0.9	11.0
UGC 04904			1670	15.0	5.3	2.9	33.9
NGC 2805	B	3.4	1733	11.5			SDSS
NGC 2814			1592	14.3	10.6	3.1	65.3
NGC 2820			1574	13.3	13.1	3.9	80.0
NGC 2814	C	1.2	1592	14.3			SDSS
NGC 2820A			1534	15.4	2.2	1.8	13.0
NGC 2820			1574	13.3	3.7	3.1	22.6
NGC 2820	C	3.7	1574	13.3			SDSS
NGC 2820A			1534	15.4	2.0	0.6	12.1
NGC 2814			1592	14.3	3.7	1.0	22.9
NGC 2805			1733	11.5	13.1	3.6	88.1
NGC 2853		1.7	1765	14.4			DR8
NGC 2852			1773	14.1	2.2	1.3	15.3
NGC 2854		1.3	2771	13.8			SDSS
NGC 2856			2638	14.1	3.4	2.6	35.0
NGC 2968	C	2.6	1566	12.9			SDSS
NGC 2970			1618	14.4	5.0	1.9	31.1
NGC 3018	C	1.2	1863	14.1			SDSS
NGC 3023			1879	13.9	2.8	2.3	20.3
NGC 3020	B	2.3	1440	12.6			SDSS

¹¹ KPG 186

Table 3. Continued.

Galaxy	Inter.	D_{25} (')	Vel. (km/s)	mag.	Separation (D_{25})		Optical
					($'$)	(kpc)	
NGC 3024			1415	13.8	5.8	2.5	31.9
NGC 3023	B	1.8	1879	13.9			SDSS
NGC 3018			1863	14.1	2.8	1.6	20.1
NGC 3024		1.5	1415	13.8			SDSS
SDSS J095036.25+124832.6			1335	16.7	3.4	2.3	17.5
NGC 3020			1440	12.6	5.8	3.9	32.5
NGC 3031		21.4	-34	7.9			SDSS
NGC 3077			14	10.6	46.4	2.2	2.5
NGC 2976			3	10.8	82.7	3.9	1.0
NGC 3065		1.8	2000	13.5			
NGC 3066			2049	13.6	3.0	1.6	23.4
NGC 3066	C	1.2	2049	13.6			
NGC 3065			2000	13.5	3.0	2.5	22.9
NGC 3079	C	8.1	1116	11.5			SDSS
NGC 3073			1155	14.1	10.0	1.2	44.5
NGC 3118		2.1	1342	14.1			SDSS
UGC 05446			1362	15.3	9.8	4.7	51.5
NGC 3166		4.5	1345	11.3			SDSS
NGC 3169			1238	11.1	7.8	1.7	37.1
NGC 3169	B	4.4	1238	11.1			SDSS
NGC 3166			1345	11.3	7.8	1.8	40.3
NGC 3187	C	2.2	1581	13.8			SDSS
NGC 3193			1399	11.8	8.7	3.9	47.0
NGC 3190	C	3.6	1271	12.1			SDSS
NGC 3193			1399	11.8	5.8	1.6	31.4
NGC 3185			1217	12.9	10.7	3.0	50.3
NGC 3193		2.4	1399	11.8			SDSS
NGC 3190			1271	12.1	5.8	2.4	28.5
NGC 3187			1581	13.8	8.7	3.6	53.1
NGC 3220		1.2	1170	14.3			SDSS
KUG 1020+571			1224	16.0	6.0	5.0	28.2
NGC 3226	C	3.2	1151	12.3			DR8
NGC 3227			1157	11.1	2.2	0.7	9.7
NGC 3227 ¹²	A	4.0	1157	11.1			SDSS
NGC 3226			1151	12.3	2.2	0.5	9.7
NGC 3245A		2.3	1322	14.7			SDSS
SDSS J102716.85+283039.6			1254	17.3	8.4	3.7	40.9
NGC 3245			1314	11.9	8.8	3.8	44.6
NGC 3329		1.9	1948	13.0			
UGC 05841			1766	14.8	7.3	3.9	50.2
NGC 3368		8.5	897	10.1			SDSS
MESSIER 095			778	11.4	41.7	4.9	125.5
NGC 3377		3.9	665	11.2			DR8
NGC 3377A			573	14.2	7.0	1.8	15.5
NGC 3377A		1.4	573	14.2			SDSS
NGC 3377			665	11.2	7.0	5.0	17.9
NGC 3395 ¹³	A	1.7	1625	12.4			SDSS
NGC 3396			1625	13.0	1.1	0.7	7.2
NGC 3396 ¹³	A	3.1	1625	13.0			SDSS
NGC 3395			1625	12.4	1.1	0.4	7.2
IC 2608			1677	15.1	14.0	4.5	91.0
IC 2604			1633	14.3	14.5	4.7	91.7
NGC 3414		2.7	1414	12.0			SDSS
NGC 3418			1268	13.7	8.4	3.1	41.1
NGC 3424		3.2	1494	13.2			SDSS
NGC 3430			1586	12.2	6.0	1.9	37.1
NGC 3430	C	4.0	1586	12.2			SDSS

¹² Arp 094¹³ Arp 270

Table 3. Continued.

Galaxy	Inter.	D_{25} (')	Vel. (km/s)	mag.	Separation			Optical
					(')	D_{25}	(kpc)	
NGC 3424			1494	13.2	6.0	1.5	34.9	
NGC 3440	C	2.0	1904	14.0				SDSS
NGC 3445			2069	12.9	9.9	5.0	79.2	
NGC 3447A	B	1.4	1066	13.1				SDSS
NGC 3447b			1098	14.3	1.6	1.1	6.7	
NGC 3454	C	2.5	1101	14.2				SDSS
NGC 3455			1102	13.3	3.6	1.4	15.2	
SDSS J105506.66+172745.4			1158	16.9	11.3	4.5	50.7	
NGC 3455		2.3	1102	13.3				SDSS
NGC 3454			1101	14.2	3.6	1.6	15.2	
NGC 3471		1.7	2109	13.1				SDSS
MCG +10-16-040			2162	15.9	2.4	1.4	19.7	
NGC 3501		4.4	1130	13.5				SDSS
NGC 3507			979	11.7	12.6	2.9	47.7	
NGC 3504		2.5	1525	11.7				SDSS
NGC 3512			1376	13.0	12.1	4.8	64.1	
NGC 3507		2.9	979	11.7				SDSS
NGC 3501			1130	13.5	12.6	4.3	55.1	
NGC 3511	C	6.0	1109	11.5				
NGC 3513			1194	11.9	10.8	1.8	49.9	
NGC 3513		2.8	1194	11.9				
NGC 3511			1109	11.5	10.8	3.9	46.4	
NGC 3607		4.6	960	10.8				DR8
NGC 3599			832	12.8	21.1	4.6	68.0	
NGC 3617		1.8	2167	13.7				DR8
ESO 503- G 011			2047	15.4	5.9	3.3	46.3	
NGC 3623		7.6	807	10.2				SDSS
MESSIER 066			727	9.7	20.2	2.7	56.7	
NGC 3628			843	10.2	35.8	4.7	116.6	
NGC 3625	C	1.7	1940	14.0				SDSS
UGC 06344			1934	16.8	2.6	1.5	19.6	
UGC 06369			1913	16.2	7.5	4.4	55.5	
NGC 3627	B	10.2	727	9.7				SDSS
MESSIER 065			807	10.2	20.2	2.0	63.0	
NGC 3628			843	10.2	35.9	3.5	117.0	
NGC 3628	B	11.0	843	10.2				SDSS
MESSIER 065			807	10.2	35.8	3.3	111.6	
MESSIER 066			727	9.7	35.9	3.3	100.9	
NGC 3636		2.5	1741	12.8				DR8
NGC 3637			1846	13.2	3.9	1.5	27.6	
NGC 3637		2.5	1846	13.2				SDSS
NGC 3636			1741	12.8	3.9	1.5	26.0	
NGC 3656	B	1.5	2890	13.3				DR8
SBS 1120+540			2784	16.0	4.7	3.1	50.3	
NGC 3664	B	1.4	1381	13.2				SDSS
NGC 3664A			1326	14.9	6.2	4.4	31.6	
NGC 3672		2.9	1862	12.2				SDSS
KUG 1122-093			1968	14.6	13.5	4.7	102.7	
NGC 3686		3.0	1156	11.9				SDSS
NGC 3684			1163	12.0	14.0	4.7	63.1	
NGC 3712		2.0	1580	14.9				SDSS
SDSS J113119.85+283125.0			1499	16.8	3.5	1.8	20.6	
NGC 3718	B	4.7	993	11.6				SDSS
NGC 3729			1060	12.0	11.7	2.5	48.0	
NGC 3729	C	2.9	1060	12.0				SDSS
NGC 3718			993	11.6	11.7	4.0	44.9	
NGC 3735		3.5	2696	12.5				DR8
UGC 06532			2608	15.1	16.5	4.7	166.3	
NGC 3769	C	2.9	737	12.5				SDSS
NGC 3769A			734	14.7	1.4	0.5	4.0	

Table 3. Continued.

Galaxy	Inter.	D_{25} (')	Vel. (km/s)	mag.	Separation (D_{25})		Optical
					($'$)	(kpc)	
NGC 3786	C	2.0	2678	13.5			SDSS
NGC 3788			2699	13.4	1.4	0.7	14.5
NGC 3788	C	2.0	2699	13.4			SDSS
NGC 3786			2678	13.5	1.4	0.7	14.4
NGC 3838		1.4	1320	13.2			DR8
CGCG 292-024			1282	15.9	6.8	4.8	33.6
NGC 3893	C	2.7	967	11.2			SDSS
NGC 3896			905	13.9	3.7	1.4	13.0
NGC 3896		1.4	905	13.9			SDSS
NGC 3893			967	11.2	3.7	2.6	13.9
NGC 3917		4.6	965	12.5			SDSS
NGC 3917A			837	13.9	11.4	2.5	37.0
UGC 06840			1046	14.3	21.1	4.6	85.5
NGC 3936		4.0	2013	12.8			
ESO 504- G 024			1894	15.1	18.1	4.5	132.2
NGC 3972		3.7	852	13.1			SDSS
NGC 3990			696	13.4	17.7	4.8	47.7
NGC 3981	B	3.3	1723	12.1			
ESO 572- G 023			1805	13.8	12.1	3.7	84.5
NGC 4026		4.4	930	11.7			DR8
UGC 06992			752	14.6	20.4	4.7	59.3
NGC 4030		3.8	1465	11.6			SDSS
UGC 07000			1492	14.4	16.7	4.4	96.5
NGC 4038 ¹⁴	A	5.4	1642	11.2			
NGC 4039			1641	11.1	1.1	0.2	7.1
NGC 4039 ¹⁴	A	5.4	1641	11.1			
NGC 4038			1642	11.2	1.1	0.2	7.1
NGC 4041		2.4	1234	12.1			SDSS
UGC 07009			1119	14.4	11.8	4.9	51.0
NGC 4088	C	7.1	757	11.2			SDSS
NGC 4085			746	12.9	11.3	1.6	32.6
NGC 4106 ¹⁵	A	4.2	2150	12.4			
2MASX J12065029-2936236			1979	15.3	9.8	2.3	74.8
IC 2996			2256	14.2	17.2	4.1	150.5
NGC 4108		1.6	2513	13.0			SDSS
NGC 4108B			2673	14.6	5.1	3.2	52.3
NGC 4108B	C	1.3	2673	14.6			SDSS
NGC 4108			2513	13.0	5.1	3.9	49.1
NGC 4111		1.8	807	11.6			SDSS
NGC 4117			934	13.7	8.6	4.8	31.2
NGC 4123		3.2	1327	12.9			SDSS
NGC 4116			1309	12.4	14.1	4.4	71.4
NGC 4145		4.7	1009	11.8			SDSS
NGC 4145A			1168	14.7	12.7	2.7	57.3
NGC 4157		6.2	774	12.2			SDSS
MCG +08-22-082			899	15.0	13.2	2.1	46.0
NGC 4197		2.8	2064	13.4			SDSS
VCC 0114			2071	16.0	7.8	2.8	62.2
HARO 06			2019	14.9	10.2	3.7	80.0
NGC 4216		7.8	131	11.0			SDSS
NGC 4222			230	13.9	11.7	1.5	10.4
NGC 4220		3.3	914	12.2			SDSS
NGC 4218			730	13.8	15.4	4.7	43.6
NGC 4222		2.8	230	13.9			SDSS
VCC 0165			255	14.9	9.0	3.2	8.9
NGC 4216			131	11.0	11.7	4.2	5.9
NGC 4235		3.8	2410	12.5			SDSS

¹⁴ Arp 244¹⁵ Pair AM 1204-292. NGC 4105 has been excluded ($\Delta V = 214$ km/s).

Table 3. Continued.

Galaxy	Inter.	D_{25} (')	Vel. (km/s)	mag.	Separation		Optical
					(')	D_{25}	
NGC 4224			2603	12.8	18.5	4.9	186.6
NGC 4256		3.9	2528	12.7			SDSS
CGCG 315-030			2679	14.9	12.3	3.1	127.3
NGC 4259		1.0	2401	14.2			DR8
VCC 0338			2421	16.5	5.4	5.3	51.0
NGC 4260	C	2.5	1958	12.5			SDSS
NGC 4269			2074	13.9	8.4	3.3	67.1
NGC 4261		4.3	2238	11.4			DR8
IC 3155			2292	14.4	12.1	2.8	107.6
NGC 4269			2074	13.9	13.1	3.1	105.0
NGC 4268		1.5	2374	13.3			SDSS
NGC 4273			2378	12.6	4.2	2.8	38.6
NGC 4277			2196	14.2	5.4	3.6	45.6
NGC 4270		1.9	2357	12.7			DR8
NGC 4273			2378	12.6			
NGC 4277			2196	14.2	1.9	0.9	16.2
NGC 4268			2374	13.3	4.2	1.9	38.5
NGC 4270			2357	12.7	7.4	3.4	67.4
NGC 4259			2401	14.2	8.7	3.9	80.4
NGC 4273	B	2.2	2378	12.6			SDSS
NGC 4277			2196	14.2			
NGC 4268			2374	13.3			
NGC 4270			2357	12.7			
NGC 4259			2401	14.2			
NGC 4278		2.9	649	11.2			SDSS
NGC 4286			644	14.2	8.6	3.0	21.5
NGC 4294		2.7	355	12.5			SDSS
NGC 4299			232	12.9	5.6	2.1	5.0
NGC 4298	C	3.2	1135	12.5			SDSS
NGC 4302	C		1149	13.6	2.4	0.7	10.7
UGC 07436			985	14.5	14.6	4.6	55.7
NGC 4299		1.5	232	12.9			SDSS
NGC 4294			355	12.5	5.6	3.7	7.7
NGC 4302		6.0	1149	13.6			SDSS
NGC 4298			1135	12.5	2.4	0.4	10.5
UGC 07436			985	14.5	13.2	2.2	50.4
NGC 4306	C	1.5	1981	13.8			DR8
NGC 4305			1888	13.4	2.8	1.9	20.4
NGC 4309		1.9	869	13.6			SDSS
NGC 4309A			750	16.0	1.5	0.8	4.3
VCC 0558			914	16.4	4.9	2.6	17.5
NGC 4319	B	2.5	1476	12.8			LT
CGCG 352-027			1419	15.2	12.2	4.9	67.1
NGC 4341		1.7	922	14.0			DR8
NGC 4342			751	13.4	4.8	2.9	14.0
NGC 4342		1.3	751	13.4			DR8
NGC 4341			922	14.0	4.8	3.8	17.2
NGC 4355		1.4	2179	13.7			SDSS
VV 655 NED01			2202	15.5	3.0	2.1	25.4
NGC 4380		3.3	963	13.0			SDSS
IC 3328			1025	14.5	9.1	2.8	36.0
NGC 4382	C	6.9	729	10.0			DR8
NGC 4394			922	11.7	7.6	1.1	27.0
NGC 4394	C	3.5	922	11.7			SDSS
MESSIER 085			729	10.0	7.6	2.2	21.4
NGC 4402		3.5	232	12.6			SDSS
IC 3355			162	15.2	11.2	3.2	7.0
NGC 4411A		1.7	1278	13.4			SDSS
NGC 4411b			1272	12.9	4.3	2.5	21.1
NGC 4411B		1.9	1272	12.9			SDSS
NGC 4411			1278	13.4	4.3	2.3	21.2
NGC 4417		3.1	854	12.0			DR8

Table 3. Continued.

Galaxy	Inter.	D_{25} (')	Vel. (km/s)	mag.	Separation		Optical
					(')	D_{25}	
SDSS J122649.07+093427.8			906	14.1	0.7	0.2	2.5
NGC 4428		1.7	2978	13.1			LT
NGC 4433			3000	12.9	7.1	4.2	82.4
NGC 4436		1.7	1124	14.0			DR8
NGC 4431			934	13.7	3.7	2.2	13.4
NGC 4438 ¹⁶	B	9.1	71	11.0			SDSS
NGC 4402			232	12.6	24.7	2.7	22.1
NGC 4407			102	12.2	29.8	3.3	11.8
NGC 4454		2.2	2407	13.2			SDSS
CGCG 014-047			2421	15.6	7.3	3.3	68.3
NGC 4478		1.7	1349	12.4			DR8
MESSIER 087			1307	9.6	8.7	5.0	43.8
NGC 4485	B	2.0	493	12.3			SDSS
NGC 4490			565	10.2	3.6	1.8	7.8
NGC 4486		7.1	1307	9.6			DR8
NGC 4478			1349	12.4	8.7	1.2	45.2
NGC 4490	B	6.8	565	10.2			SDSS
NGC 4485			493	12.3	3.6	0.5	6.8
NGC 4498		2.8	1507	12.8			SDSS
NGC 4502			1626	14.6	11.4	4.1	71.8
NGC 4503		3.5	1342	12.1			SDSS
IC 3470			1505	14.4	6.7	1.9	38.9
NGC 4527		6.3	1736	11.4			SDSS
NGC 4533			1753	14.2	20.0	3.2	135.5
NGC 4536			1808	11.2	28.3	4.5	198.0
NGC 4532	C	2.5	2012	12.2			SDSS
Holmberg VII			2039	14.6	11.9	4.8	94.0
NGC 4536		7.1	1808	11.2			SDSS
NGC 4527			1736	11.4	28.3	4.0	190.1
NGC 4548	C	5.5	486	11.0			SDSS
NGC 4571			342	11.8	27.5	5.0	36.3
NGC 4550		3.2	381	12.3			SDSS
VCC 1627			236	15.0	9.8	3.1	9.0
NGC 4552		8.1	340	10.7			DR8
NGC 4550			381	12.3	20.3	2.5	29.8
NGC 4565		17.0	1230	10.4			SDSS
NGC 4494			1344	10.7	67.9	4.0	353.0
NGC 4567 ¹⁷	A	2.8	2247	12.6			SDSS
NGC 4568			2255	12.5	1.2	0.4	10.5
NGC 4568 ¹⁷	A	4.3	2255	12.5			SDSS
NGC 4567			2247	12.6	1.2	0.3	10.5
NGC 4593	C	2.4	2698	11.7			LT
MCG -01-32-033			2549	13.9	3.8	1.6	37.5
NGC 4596		3.9	1870	11.3			SDSS
NGC 4608			1864	12.0	19.1	4.9	137.5
NGC 4597		3.5	1039	12.6			SDSS
LCRS B123647.4-052325			1199	15.2	15.0	4.3	69.4
NGC 4618	C	3.5	544	11.2			SDSS
NGC 4625			598	13.2	8.3	2.4	19.2
NGC 4628	C	1.7	2828	12.8			SDSS
NGC 4626			2896	14.1	4.4	2.6	49.2
NGC 4631		14.5	606	9.8			SDSS
NGC 4656 NED01			664	10.6	32.1	2.2	82.5
NGC 4633	C	1.8	291	13.8			SDSS
NGC 4634	C		297	13.2	3.8	2.1	4.3
NGC 4634		2.5	297	13.2			SDSS
NGC 4633			291	13.8	3.8	1.5	4.3

¹⁶ NGC 4435 has been excluded ($\Delta V = 730$ km/s).¹⁷ KPG 347A

Table 3. Continued.

Galaxy	Inter.	D_{25} (')	Vel. (km/s)	mag.	Separation		Optical
					(')	D_{25}	
NGC 4649		6.8	1117	9.8			DR8
NGC 4638			1164	12.1	14.5	2.1	65.1
NGC 4660			1083	12.2	25.2	3.7	105.5
NGC 4653		2.3	2631	13.4			SDSS
NGC 4642			2644	13.7	9.7	4.2	98.8
NGC 4654	C	4.7	1046	12.0			SDSS
NGC 4639			1018	12.2	17.5	3.7	68.8
NGC 4666		5.0	1529	11.5			SDSS
NGC 4668			1636	13.5	7.3	1.5	46.4
NGC 4668		1.6	1636	13.5			SDSS
NGC 4666			1529	11.5	7.3	4.6	43.4
NGC 4688	C	3.7	986	12.6			SDSS
CGCG 043-029			1041	15.5	6.7	1.8	27.0
NGC 4725		9.8	1206	10.1			SDSS
NGC 4747			1190	13.0	24.4	2.5	112.2
NGC 4731	B	6.3	1489	11.9			LT
NGC 4731A			1514	13.5	10.4	1.7	61.1
NGC 4762		8.3	984	11.1			SDSS
NGC 4733			928	12.7	32.9	4.0	118.2
NGC 4772		4.1	1040	12.0			SDSS
CGCG 015-036			859	14.6	18.5	4.5	61.5
NGC 4795	C	2.2	2781	12.1			SDSS
UGC 08042			2659	14.8	9.0	4.1	92.5
UGC 08045			2801	14.9	10.7	4.9	115.7
NGC 4809 ¹⁸	A	1.6	915	14.3			SDSS
NGC 4810			912	14.2	0.8	0.5	2.9
NGC 4866		5.8	1988	12.1			SDSS
UGC 08085			2047	14.3	28.7	4.9	227.0
NGC 4902		2.7	2673	11.6			
NGC 4887			2687	14.1	10.4	3.9	108.2
NGC 4948		2.2	1123	14.0			
DDO 163			1123	16.0	5.7	2.6	24.9
NGC 4958		4.7	1455	12.1			LT
NGC 4948A			1541	14.5	13.6	2.9	81.1
NGC 4961		1.1	2535	14.0			SDSS
LSBC D508-01			2527	17.0	1.5	1.3	14.4
NGC 4968		2.3	2957	13.9			DR8
ESO 508- G 010			3140	14.8	9.4	4.1	113.6
NGC 4997		1.6	2376	13.5			DR8
MCG -03-34-004			2569	14.5	5.5	3.4	54.7
NGC 5018	B	3.5	2816	12.9			
NGC 5022			3001	14.0	7.2	2.1	83.7
ESO 576- G 008			2691	14.9	10.8	3.1	112.7
NGC 5022		2.5	3001	14.0			
NGC 5018			2816	12.9	7.2	2.9	78.6
NGC 5030		1.8	2397	13.8			DR8
2MASXi J1313594-162303			2493	15.9	6.5	3.7	62.9
NGC 5033		9.8	875	10.8			SDSS
Holmberg VIII			944	13.5	22.7	2.3	82.8
NGC 5005			946	10.6	41.2	4.2	150.6
NGC 5044		3.6	2782	11.8			DR8
NGC 5037			2966	12.2	13.6	3.8	156.3
NGC 5049	C	2.0	3023	13.7			DR8
2MASX J13153203-1628509			3208	15.8	8.2	4.1	102.2
NGC 5054	C	5.0	1741	11.7			
NGC 5047			1881	13.5	18.2	3.6	132.0
NGC 5073		3.8	2744	13.5			
MCG -02-34-033			2853	15.5	13.8	3.6	151.7

¹⁸ Arp 277

Table 3. Continued.

Galaxy	Inter.	D_{25} (')	Vel. (km/s)	mag.	Separation			Optical
					(')	D_{25}	(kpc)	
IC 4221			2889	13.6	18.6	4.9	208.3	
NGC 5076	C	1.3	2991	13.5				DR8
NGC 5077			2806	12.4	5.0	3.7	54.7	
NGC 5077		2.6	2806	12.4				DR8
NGC 5076			2991	13.5	5.0	1.9	58.3	
NGC 5084	C	10.0	1721	11.4				DR8
LEDA 158715			1894	13.8	11.7	1.2	85.4	
UGCA 348			1627	13.2	27.7	2.8	174.2	
NGC 5109		1.6	2131	13.8				SDSS
SDSS J132123.99+574140.3			2046	15.1	5.2	3.2	41.0	
NGC 5112	C	3.0	975	13.4				SDSS
NGC 5107			946	13.8	13.3	4.4	48.8	
NGC 5169		1.5	2436	14.0				SDSS
NGC 5173			2419	13.5	5.5	3.7	51.4	
SDSS J132836.15+464604.0			2478	16.8	7.3	4.9	69.7	
NGC 5170		8.7	1501	12.3				
MCG -03-34-082			1448	13.6	31.0	3.6	173.4	
6dF J1327262-173918			1647	15.1	38.7	4.5	246.6	
NGC 5173		1.1	2419	13.5				SDSS
NGC 5169			2436	14.0	5.5	5.0	51.7	
NGC 5194 ¹⁹	A	7.8	463	9.0				LT
MESSIER 051b			465	10.4	4.4	0.6	7.9	
NGC 5195 ¹⁹	A	5.5	465	10.4				
MESSIER 051a			463	9.0	4.4	0.8	7.9	
NGC 5216	B	1.7	2939	13.6				SDSS
NGC 5218			2933	13.2	4.0	2.4	45.9	
NGC 5218		1.9	2933	13.2				SDSS
NGC 5216			2939	13.6	4.0	2.1	45.9	
NGC 5290		4.7	2573	12.6				SDSS
NGC 5289			2526	14.0	12.7	2.7	124.1	
NGC 5297	C	3.7	2409	12.5				SDSS
NGC 5296			2254	14.9	1.6	0.4	13.5	
NGC 5311		1.9	2698	13.3				SDSS
NGC 5313			2538	12.6	9.2	4.9	90.7	
NGC 5313		2.8	2538	12.6				SDSS
NGC 5311			2698	13.3	9.2	3.3	96.4	
NGC 5326		2.2	2520	12.7				SDSS
IC 4336			2530	14.3	8.0	3.7	78.6	
NGC 5346		1.5	2519	14.3				SDSS
2MASX J13522492+3933269			2703	16.0	7.3	4.8	76.0	
NGC 5348		3.9	1451	13.9				SDSS
NGC 5356			1374	13.3	13.4	3.4	71.0	
SDSS J135502.70+050525.2			1396	16.6	15.2	3.9	82.2	
NGC 5350	C	2.7	2321	12.2				SDSS
NGC 5355			2344	13.9	4.8	1.8	43.5	
NGC 5353			2325	12.0	5.0	1.8	44.5	
NGC 5358			2401	14.3	9.0	3.3	83.9	
NGC 5353 ²⁰	A	2.4	2325	12.0				SDSS
NGC 5355			2344	13.9	4.9	2.0	44.5	
NGC 5350			2321	12.2	5.0	2.1	44.4	
NGC 5358			2401	14.3	6.4	2.7	59.8	
NGC 5354 ²⁰	A	3.0	2579	12.3				SDSS
NGC 5358			2401	14.3	6.6	2.2	61.3	
NGC 5355		1.1	2344	13.9				SDSS
NGC 5358			2401	14.3	4.6	4.2	43.1	
NGC 5355			2321	12.2	4.8	4.4	43.1	
NGC 5350			2325	12.0	4.9	4.5	44.1	

¹⁹ Arp 085²⁰ Triplet KTG 50

Table 3. Continued.

Galaxy	Inter.	D_{25} (')	Vel. (km/s)	mag.	Separation (') D_{25}		Optical
					(kpc)		
NGC 5356		2.8	1374	13.3			SDSS
NGC 5348			1451	13.9	13.4	4.8	75.0
NGC 5358		1.1	2401	14.3			DR8
NGC 5355			2344	13.9	4.6	4.1	42.1
NGC 5363		4.7	1139	11.1			SDSS
NGC 5364			1241	11.2	14.5	3.1	69.4
NGC 5364		3.8	1241	11.2			SDSS
NGC 5360			1171	14.1	8.5	2.2	38.3
NGC 5363			1139	11.1	14.5	3.8	63.7
NGC 5379	C	2.0	1607	13.9			DR8
UGC 08859			1610	15.8	7.3	3.6	45.7
NGC 5403		2.8	2746	13.7			SDSS
UGC 08919 NOTES01			2730	14.7	1.6	0.6	17.3
NGC 5426 ²¹	A	3.1	2572	12.7			
NGC 5427			2618	11.9	2.3	0.8	23.5
LCRS B140059.8-055011			2609	13.5	3.1	1.1	30.9
NGC 5427 ²¹	A	3.6	2618	11.9			
NGC 5426			2572	12.7	2.3	0.6	23.1
LCRS B140059.8-055011			2609	13.5	3.9	1.1	38.8
NGC 5457		24.0	241	8.3			SDSS
NGC 5474			273	11.3	44.2	1.8	46.7
NGC 5468		2.3	2842	12.4			LT
NGC 5472			2910	14.8	5.0	2.2	56.6
NGC 5472		1.4	2910	14.8			LT
NGC 5468			2842	12.4	5.0	3.6	55.3
NGC 5485		2.5	2000	12.4			DR8
NGC 5484			2030	15.3	3.7	1.5	29.2
NGC 5506	C	2.9	1853	12.8			SDSS
NGC 5507			1844	13.6	3.7	1.3	26.6
NGC 5507		1.6	1844	13.6			SDSS
NGC 5506			1853	12.8	3.7	2.3	26.8
NGC 5520		1.4	1877	13.2			SDSS
SBS 1410+504			1815	16.1	6.6	4.7	46.5
NGC 5529		5.8	2875	12.9			SDSS
NGC 5544			3040	14.0	27.3	4.7	320.9
NGC 5560 ²²	B	3.5	1729	13.2			SDSS
NGC 5569			1780	14.9	6.9	2.0	47.5
NGC 5574		1.3	1659	13.0			SDSS
NGC 5576			1487	11.8	2.8	2.1	15.9
NGC 5576		2.8	1487	11.8			SDSS
NGC 5574			1659	13.0	2.8	1.0	17.7
NGC 5577			1489	13.1	10.2	3.6	58.5
NGC 5577		2.8	1489	13.1			SDSS
NGC 5576			1487	11.8	10.2	3.6	58.4
NGC 5574			1659	13.0	12.6	4.5	80.9
NGC 5582		2.2	1362	12.5			DR8
UGC 09194			1307	15.4	12.8	5.9	64.8
NGC 5595	B	2.1	2711	13.1			
NGC 5597			2683	12.6	4.2	2.0	43.1
NGC 5597	B	2.0	2683	12.6			
NGC 5595			2711	13.1	4.2	2.1	43.5
NGC 5636		1.4	1745	14.1			SDSS
NGC 5638			1676	12.2	2.0	1.4	13.0
UGC 09310			1846	14.5	6.2	4.4	43.9
NGC 5638		1.9	1676	12.2			DR8
NGC 5636			1745	14.1	2.0	1.0	13.5
UGC 09310			1846	14.5	5.2	2.7	37.3

²¹ Arp 271²² NGC 5566 has been excluded ($\Delta V = 222$ km/s).

Table 3. Continued.

Galaxy	Inter.	D_{25} (')	Vel. (km/s)	mag.	Separation		Optical
					(')	D_{25}	
NGC 5661	B	1.2	2354	14.2			SDSS
VIII Zw 432			2369	16.7	4.5	3.8	41.4
NGC 5689		3.6	2160	12.8			SDSS
NGC 5682			2273	14.5	8.5	2.4	75.0
NGC 5693			2281	14.1	11.6	3.2	102.6
NGC 5707		2.4	2212	13.1			SDSS
SBS 1435+516			2381	15.8	9.3	3.9	85.6
NGC 5713	B	2.5	1899	12.2			SDSS
NGC 5719			1733	12.8	11.3	4.5	76.1
NGC 5719	B	3.1	1733	12.8			SDSS
NGC 5713			1899	12.2	11.3	3.7	83.3
NGC 5730	C	2.0	2533	14.2			SDSS
NGC 5731			2537	14.1	3.8	1.9	37.7
NGC 5731	C	1.5	2537	14.1			SDSS
NGC 5730			2533	14.2	3.8	2.6	37.6
NGC 5740	C	2.7	1572	12.8			SDSS
NGC 5738			1746	14.5	8.4	3.1	56.4
NGC 5746		7.2	1724	11.3			SDSS
NGC 5740			1572	12.8	18.3	2.5	111.2
NGC 5757	C	2.1	2677	13.5			
ESO 580-G 034			2796	15.5	3.6	1.7	39.2
NGC 5774	C	1.7	1555	13.7			SDSS
NGC 5775			1681	12.2	4.4	2.6	28.7
IC 1070			1677	15.3	6.3	3.7	40.6
NGC 5775		3.7	1681	12.2			SDSS
NGC 5774			1555	13.7	4.4	1.2	26.5
IC 1067			1577	13.5	18.3	4.9	111.4
NGC 5777		3.0	2145	14.1			SDSS
UGC 09570			2205	15.6	2.7	0.9	23.4
NGC 5796		2.6	2863	12.7			DR8
6dF J1459410-164235			2857	14.5	6.5	2.5	72.3
NGC 5812		2.7	1970	12.2			DR8
IC 1084			2158	15.1	4.9	1.8	40.6
NGC 5821	C	1.5	3376	14.6			SDSS
NGC 5820			3335	13.4	3.7	2.5	47.4
NGC 5838		3.9	1359	11.9			DR8
NGC 5841			1244	14.2	18.1	4.7	87.0
NGC 5899	B	2.1	2562	12.5			SDSS
NGC 5900			2511	14.8	9.6	4.6	93.0
NGC 5915	B	1.7	2272	13.0			DR8
NGC 5916A			2292	14.6	4.7	2.8	41.8
NGC 5916			2256	14.2	4.8	2.8	41.9
NGC 5916	B	3.1	2256	14.2			DR8
NGC 5915			2272	13.0	4.8	1.5	42.2
NGC 5916A			2292	14.6	7.2	2.3	63.5
NGC 5916A	B	1.4	2292	14.6			DR8
NGC 5915			2272	13.0	4.7	3.4	41.4
NGC 5930 ²³	A	1.7	2616	13.3			SDSS
NGC 5929			2492	13.9	0.5	0.3	4.5
NGC 5953 ²⁴	A	1.5	1965	13.0			SDSS
NGC 5954			1959	13.7	0.7	0.5	5.6
NGC 5954 ²⁴	A	1.0	1959	13.7			SDSS
NGC 5953			1965	13.0	0.7	0.7	5.6
NGC 5962	C	2.5	1957	12.2			SDSS
UGC 09925			1916	14.7	10.1	4.0	74.7
NGC 5970	C	2.8	1957	12.2			SDSS
IC 1131			2017	14.8	8.3	3.0	64.6

²³ Arp 090²⁴ Arp 091

Table 3. Continued.

Galaxy	Inter.	D_{25} (')	Vel. (km/s)	mag.	Separation D_{25}		Optical
					(')	(kpc)	
NGC 6168		1.7	2519	14.7			SDSS
SDSS J163130.55+200537.0			2493	17.5	5.9	3.5	56.8
NGC 6255		3.1	919	13.4			DR8
HS 1653+3634 ²⁵			845	16.0	1.1	0.4	3.7
NGC 6278		1.7	2790	13.1			SDSS
NGC 6276			2754	14.8	2.3	1.4	24.7
NGC 6340		2.6	1198	11.9			SDSS
IC 1251			1210	14.2	6.4	2.5	30.1
NGC 6861		3.2	2829	12.1			DR8
IC 4943			2969	13.6	8.5	2.7	97.7
2MASX J20062917-4819434			2654	11.4	8.7	2.8	89.5
NGC 6861B			2953	15.1	13.8	4.4	157.4
NGC 6861D			2633	13.4	13.8	4.4	140.5
NGC 6868		3.6	2854	11.7			DR8
2MASX J20095889-4821262			2852	13.7	1.6	0.4	17.2
NGC 6870	C	2.5	2951	13.2	6.2	1.7	70.9
NGC 6870			2951	13.2			
2MASX J20095889-4821262			2852	13.7	4.7	1.9	51.4
NGC 6868			2854	11.7	6.2	2.5	68.5
2MASX J20090112-4819155			2963	16.0	11.8	4.7	134.9
NGC 7041		3.5	1946	12.1			DR8
ESO 235- G 083			2036	13.6	13.7	3.9	107.6
NGC 7049		4.0	2285	11.7			DR8
ESO 235- G 085			2192	13.2	7.4	1.9	63.1
NGC 7097		1.9	2616	12.6			DR8
NGC 7097A			2594	15.1	5.8	3.0	58.2
NGC 7162		3.1	2314	13.3			
NGC 7166			2466	12.8	11.0	3.5	104.8
NGC 7162A			2269	13.1	14.3	4.6	125.2
NGC 7173		1.9	2497	13.1			DR8
NGC 7174			2659	14.2	1.3	0.7	13.8
NGC 7176			2511	12.3	1.5	0.8	14.3
NGC 7176		1.1	2511	12.3			DR8
NGC 7174			2659	14.2	0.5	0.4	4.8
NGC 7173			2497	13.1	1.5	1.3	14.2
NGC 7187		1.1	2670	13.8			DR8
2MASX J22024449-3248110			2740	14.5	0.1	0.1	0.6
6dF J2202445-324811			2699	12.7	0.1	0.1	0.7
NGC 7233	C	1.8	1841	13.1			
NGC 7232			1915	12.9	1.9	1.1	14.2
NGC 7241		2.8	1447	13.4			DR8
UGC 11964			1421	16.0	5.0	1.8	27.2
NGC 7280		2.0	1844	13.0			DR8
UGCA 429			1901	15.3	4.7	2.3	34.3
NGC 7302		1.7	2703	13.6			DR8
MCG -02-57-015			2515	15.0	5.8	3.3	56.0
NGC 7307	C	3.8	2089	12.9			
ESO 345- G 027			2175	15.4	18.6	4.9	156.2
NGC 7314	C	4.2	1428	11.9			
ESO 534- G 001			1407	14.8	16.5	3.9	89.8
NGC 7463 ²⁶	C	1.6	2341	13.8			DR8
UGC 12321			2164	15.7	7.1	4.4	59.1
NGC 7465		1.1	1968	13.3			DR8
NGC 7464			1875	14.3	1.8	1.7	13.3
NGC 7484		1.1	2728	12.8			DR8
6dF J2306355-361459			2598	14.7	6.1	5.6	61.4
ESO 407- G 004			2718	15.1	7.7	7.0	81.0

²⁵ Probably not a galaxy.²⁶ NGC 7464 ($\Delta V = 466$ km/s) and NGC 7465 ($\Delta V = 373$ km/s) have been excluded.

Table 3. Continued.

Galaxy	Inter.	D_{25} (')	Vel. (km/s)	mag.	Separation (D_{25})		Optical
					($'$)	(kpc)	
NGC 7537	C	1.8	2674	13.9			DR8
NGC 7541			2689	12.4	3.2	1.8	33.1
NGC 7541	C	3.0	2689	12.4			DR8
NGC 7537			2674	13.9	3.2	1.1	32.9
NGC 7582	C	5.6	1575	11.4			
NGC 7590			1575	12.1	9.8	1.7	59.6
NGC 7599			1651	12.1	12.7	2.3	80.8
NGC 7552			1608	11.2	27.6	4.9	171.9
NGC 7590	C	3.0	1575	12.1			
NGC 7599			1651	12.1	5.0	1.7	31.8
NGC 7582			1575	11.4	9.8	3.3	59.6
NGC 7599	C	4.6	1651	12.1			
NGC 7590			1575	12.1	5.0	1.1	30.4
NGC 7582			1575	11.4	12.7	2.8	77.1
NGC 7694	B	1.4	2281	14.1			DR8
NGC 7695			2317	16.5	1.1	0.8	9.5
NGC 7714 ²⁷	A	2.2	2798	13.0			LT
NGC 7715			2771	14.7	2.0	0.9	21.5
NGC 7715 ²⁷	A	2.0	2771	14.7			LT
NGC 7714			2798	13.0	2.0	1.0	21.8
NGC 7727	B	3.6	1868	11.5			
NGC 7724			1927	13.9	12.1	3.4	90.2
NGC 7731	C	1.0	2886	13.5			DR8
NGC 7732			2907	14.3	1.5	1.5	16.9
NGC 7732	B	1.5	2907	14.3			DR8
NGC 7731			2886	13.5	1.5	1.0	16.7
PGC 009354	C	1.6	2111	15.5			
MRK 1042			2133	16.5	7.9	4.9	65.1
PGC 012798	C	2.7	1873	15.3			
MCG -03-09-037			1866	17.0	5.3	1.9	37.9
PGC 013635		1.3	1225	14.4			DR8
ESO 358-G 056			1189	15.1	7.8	6.2	36.0
PGC 014600	C	1.9	2938	14.0			LT
MRK 0614			3030	15.1	8.7	4.6	102.4
PGC 024469	B	1.0	2115	15.0			SDSS
NGC 2648			2060	12.6	2.4	2.4	18.9
SDSS J084232.62+141717.6			2188	17.9	4.0	4.0	34.0
PGC 027825	C	1.3	1894	14.6			LT
UGCA 173			1883	15.0	5.2	4.0	37.5
PGC 028308	C	2.0	2719	14.5			
MCG -02-25-019			2580	15.0	4.7	2.3	46.7
PGC 034493		1.3	1295	15.3			DR8
SDSS J111746.30+174424.6			1464	16.8	5.1	4.0	28.6
PGC 036643	B	2.5	1705	13.5			
MRK 1306			1587	16.0	2.4	1.0	14.8
PGC 037625	A	1.5	1716	15.0			
MRK 1309 NED02			1804	13.7	0.1	0.1	0.9
MRK 1309 NED01			1589	13.7	0.2	0.1	1.1
PGC 044876		1.4	1213	15.2			DR8
6dF J1301051-052821			1095	16.1	5.3	3.6	22.3
PGC 045084		6.8	742	13.8			
UGCA 319			755	15.3	18.6	2.7	54.2
PGC 045650		2.3	2582	14.5			
2MASX J13093182-1637256			2578	16.4	3.2	1.4	32.0
PGC 046261		2.5	2651	15.0			
MCG -03-34-042			2502	15.5	1.8	0.7	17.0
2MASX J13164875-1620397			2578	14.5	6.9	2.8	69.0
LEDA 083909			2589	17.7	11.7	4.7	117.0

²⁷ Arp 284

Table 3. Continued.

Galaxy	Inter.	D_{25} (')	Vel. (km/s)	mag.	Separation (') D_{25}		Optical
					(kpc)		
PGC 049521	B	1.3	1985	13.9			SDSS
VV 099			1993	14.5	3.3	2.6	25.6
VV 099b			2070	15.5	3.4	2.6	27.4
PGC 052935 ²⁸	A	1.7	1856	14.5			
ARP 261 NED01			1834	13.3	0.8	0.5	5.7
KTS 52C			1782	15.2	5.1	3.0	34.8
PGC 052940 ²⁸	A	2.2	1834	13.3			
ARP 261 NED04			1856	14.5	0.8	0.4	5.7
KTS 52C			1782	15.2	5.7	2.6	39.1
PGC 053724		1.4	2509	14.5			
FGC 1845			2515	16.3	3.0	2.1	29.2
PGC 054817	B	1.8	1937	14.6			LT
NGC 5917			1904	14.5	4.2	2.4	31.3
PGC 068743		1.9	2828	13.2			DR8
UGCA 428			2833	14.5	8.7	4.6	94.8
PGC 069114	C	1.5	2515	15.0			
NGC 7302			2703	13.6	5.8	3.8	60.2
PGC 091408	C	1.4	2515	16.3			
MCG -02-38-030			2509	14.5	3.0	2.1	29.1
UGC 00260	C	2.1	2131	13.7			DR8
CGCG 434-012			2067	15.5	2.5	1.2	19.7
UGC 01020		1.1	2589	14.8			DR8
ESDO F611-12			2437	15.9	3.8	3.5	35.9
UGC 01176		3.9	630	14.4			DR8
UGC 01171			738	17.0	6.0	1.5	17.2
UGC 04169	B	1.5	1607	13.6			LT
UGC 04159			1591	14.1	5.2	3.5	32.1
UGC 04499	C	1.9	691	14.7			SDSS
MRK 0094			732	16.9	0.7	0.4	2.0
UGC 04704		3.6	596	15.0			SDSS
SDSS J085946.92+392305.6			588	17.2	13.8	3.8	31.5
UGC 04867		1.7	2494	14.7			SDSS
SDSS J091435.57+405523.9			2678	17.2	3.0	1.8	30.9
NGC 2785			2622	14.7	6.5	3.8	65.9
UGC 05004		1.2	1837	15.5			SDSS
SDSS J092405.24+343847.4			1914	16.5	6.0	5.0	44.1
UGC 05707	C	1.1	2800	14.8			SDSS
SDSS J103118.56+430533.7			2841	17.5	2.8	2.5	30.7
UGC 05708		3.0	1176	13.8			SDSS
SDSS J103137.27+043422.0			1202	16.2	8.5	2.8	39.4
UGC 05832	B	1.1	1216	14.0			SDSS
CGCG 065-090			1228	16.7	5.1	4.7	24.3
UGC 05841	C	1.5	1766	14.8			
NGC 3329			1948	13.0	7.3	4.9	55.3
UGC 05897	C	2.8	2718	13.8			SDSS
CGCG 066-017			2797	15.8	11.2	4.0	120.9
UGC 05898		1.3	1644	16.0			SDSS
KUG 1045+340			1612	15.4	4.4	3.4	27.3
UGC 05958		1.6	1182	15.0			SDSS
SDSS J105137.14+274919.6			1325	16.8	5.0	3.1	25.4
UGC 06309	B	1.3	2870	13.8			SDSS
MRK 1445			2799	16.1	3.5	2.7	37.8
UGC 06320		1.3	1125	13.9			SDSS
MCG +03-29-027			1140	16.1	4.0	3.1	17.5
UGC 06324	C	1.4	1068	14.4			DR8
MCG +03-29-027			1140	16.1	5.2	3.8	23.0
UGC 06320			1125	13.9	6.6	4.8	28.8
UGC 06341		1.0	1641	16.0			SDSS

²⁸ Arp 261

Table 3. Continued.

Galaxy	Inter.	D_{25} (')	Vel. (km/s)	mag.	Separation		Optical
					(')	D_{25}	
SDSS J112007.86+181802.5			1535	18.2	3.0	3.0	17.5
UGC 06355	C	1.7	2187	14.7			SDSS
2MASX J11204605+3110598			2160	15.6	2.7	1.6	22.4
UGC 06575	C	1.8	1214	14.1			SDSS
UGC 06566			1217	16.5	5.6	3.1	26.6
UGC 06969		1.3	1114	15.2			SDSS
SDSS J115834.34+532043.6			1150	17.3	5.2	4.0	22.9
UGC 07089	C	3.0	770	14.0			SDSS
UGC 07094			779	15.0	11.5	3.8	34.6
NGC 4111			807	11.6	12.8	4.3	40.0
UGC 07094		1.2	779	15.0			SDSS
SDSS J120559.63+425409.1			767	17.2	3.8	3.2	11.4
UGC 07249		1.3	622	16.1			SDSS
SDSS J121412.08+124658.4			627	17.1	6.3	4.8	15.3
UGC 07559		3.7	218	14.2			SDSS
UGC 07599			278	14.9	17.5	4.7	18.8
UGC 08040		1.5	2515	14.7			SDSS
UGC 08046			2572	15.4	2.8	1.9	27.8
PTF10icb HOST			2580	14.9	6.4	4.3	63.9
UGC 08042	B	1.1	2659	14.8			SDSS
UGC 08045			2801	14.9	3.4	3.1	36.7
UGC 08127	B	1.4	1466	15.5			SDSS
UGC 08127 NOTES01			1361	17.4	1.6	1.1	8.2
UGC 08153	C	1.7	2863	15.2			SDSS
SDSS J130249.15+035836.2			2873	18.2	4.3	2.5	47.5
UGC 08246	B	2.5	813	14.6			SDSS
MAPS-NGP O_269_1340152			850	17.4	6.1	2.4	20.1
UGC 08449	B	1.2	1212	15.5			SDSS
MCG +07-28-012			1268	16.0	4.9	4.1	23.9
UGC 09056	C	1.1	2040	14.4			SDSS
SDSS J140934.65+490239.4			1985	16.9	2.2	2.0	16.5
UGC 09310	C	1.9	1846	14.5			SDSS
NGC 5638			1676	12.2	5.2	2.8	33.9
NGC 5636			1745	14.1	6.2	3.2	41.5
UGC 09665	C	1.7	2558	14.2			SDSS
UGC 09657			2526	15.2	7.7	4.5	75.0
UGC 09760		1.8	2023	14.7			SDSS
SDSS J151208.16+013508.5			1958	17.0	6.9	3.8	52.4
UGC 09977		3.9	1915	13.9			SDSS
UGC 09979			1961	14.6	15.2	3.9	115.2
UGC 10043		2.2	2161	14.8			SDSS
MCG +04-37-035			2218	16.7	2.7	1.2	23.1
SDSS J154855.45+214533.1			2018	16.7	7.4	3.4	57.7
UGC 10049 NED03			2088	15.7	8.5	3.9	68.9
UGC 10049 NED04			2250	17.4	8.7	3.9	75.5
UGC 10806		2.1	932	13.7			LT
HERC-1:[MKK97] 308890			899	12.6	0.8	0.4	2.6
UGC 12281		3.0	2568	14.8			SDSS
KUG 2256+134			2653	16.4	7.0	2.3	71.9
SDSS J225950.41+134409.8			2622	17.3	12.0	4.0	121.6
UGC 12313	C	1.4	2028	16.0			DR8
NGC 7464			1875	14.3	6.1	4.4	44.3
UGC 12518		1.4	2787	15.5			SDSS
UGC 12522			2812	15.4	4.5	3.2	49.0
UGC 12707	B	1.3	2602	14.5			DR8
KUG 2334+171			2607	16.5	3.9	3.0	39.0

Notes. Galaxies with close companions. Column 1: name. Galaxies in boldface are S⁴G sample galaxies. Column 2 indicates whether galaxies show signs of interaction (see Sect. 6.2). Column 3 is the diameter of the galaxy, in arcmin. Column 4 and 5 are the recession velocity and optical magnitude, respectively. Columns 6-8 are the projected separation between the companion and the sample galaxy, in units of arcmin, sample galaxy diameter, and kpc, respectively. The final column, 9, indicates whether we release optical imaging for a galaxy, and from which source. All name, position, diameter, velocity and magnitude data as retrieved from the NED. A machine-readable version of the table is available from the CDS.

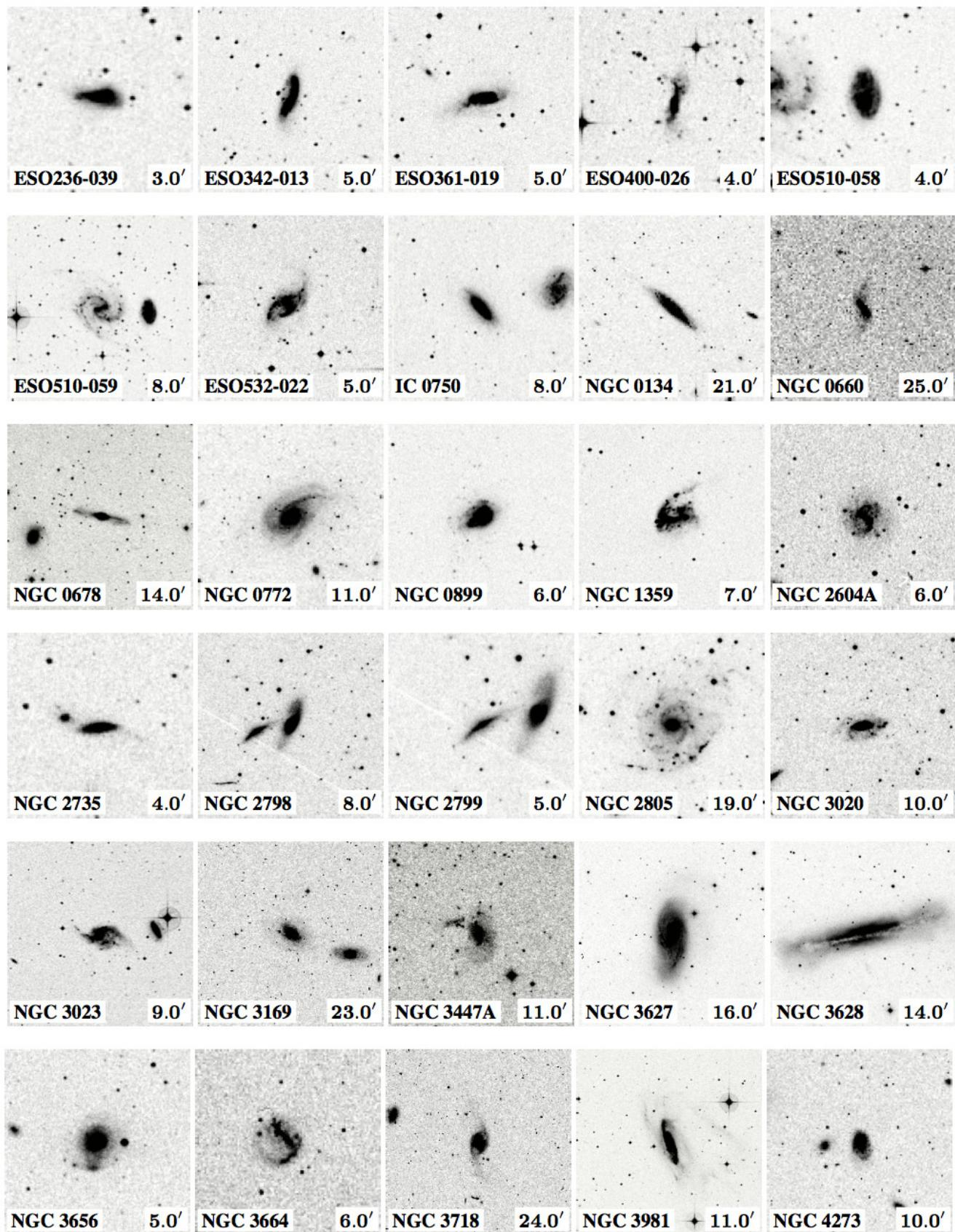
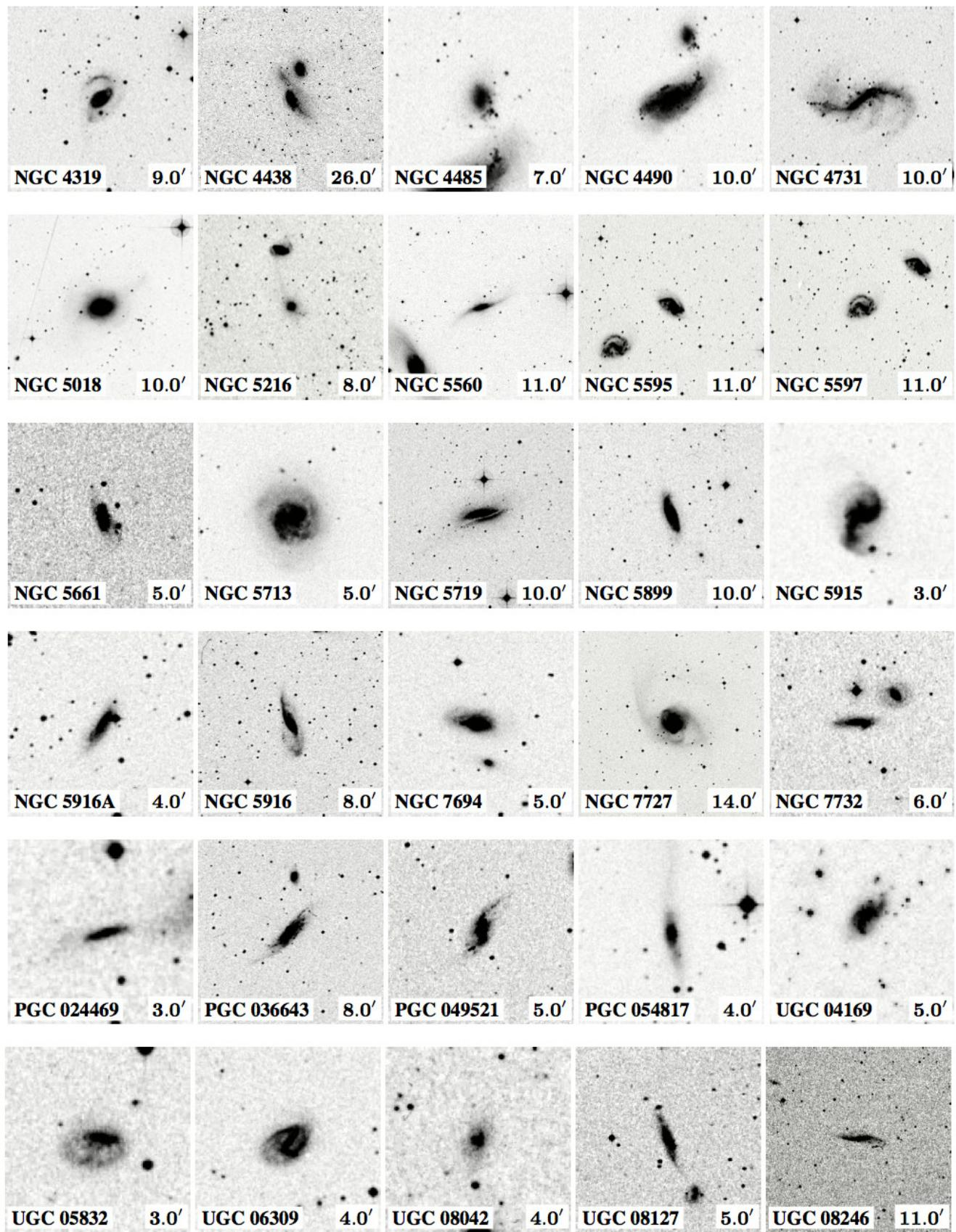


Fig. 4. As Fig. 3, now for Class B galaxies, showing significant signs of interaction.

**Fig. 4.** Continued.

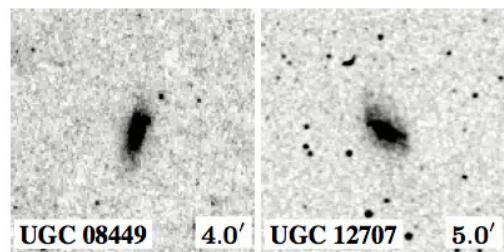


Fig. 4. Continued.

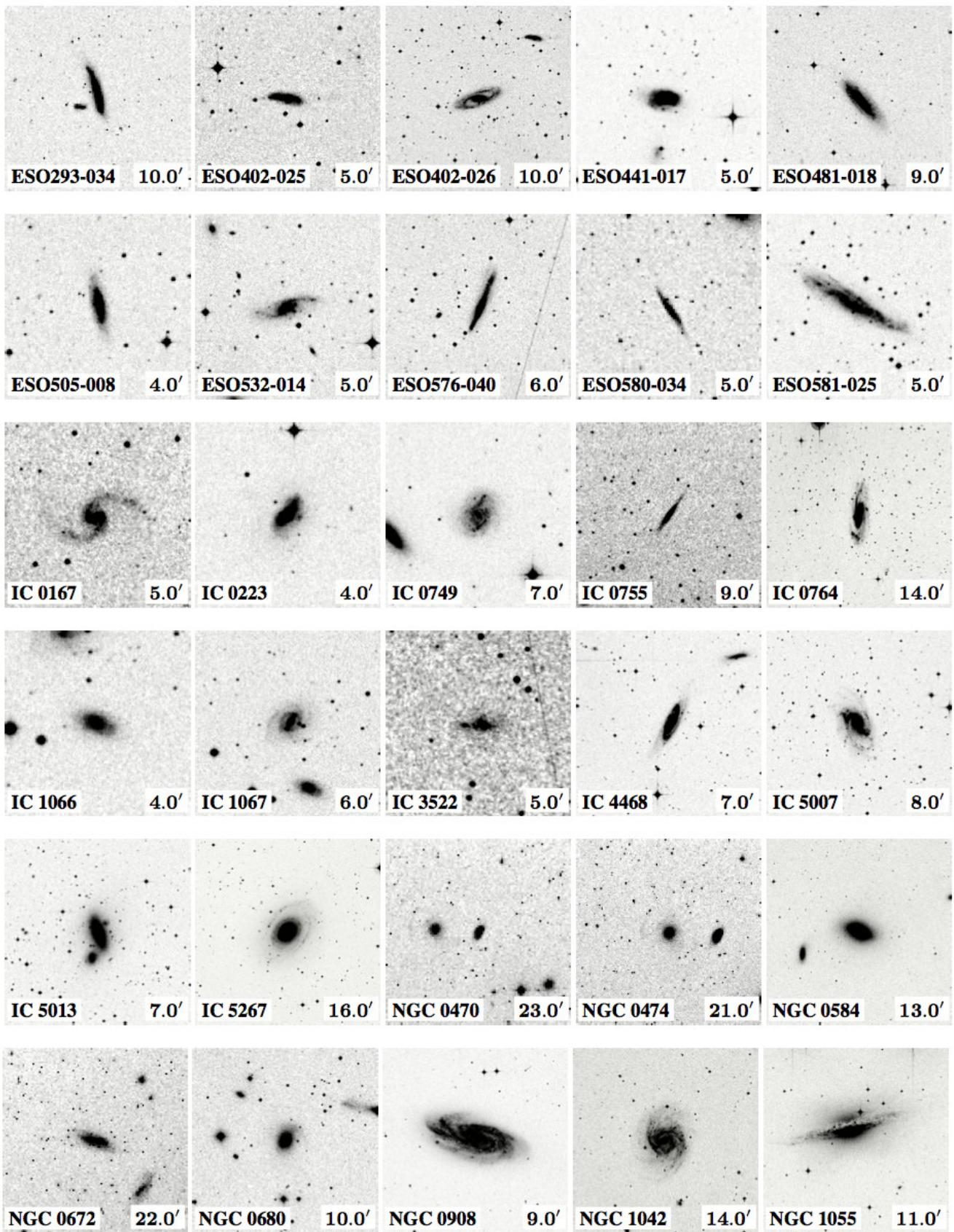


Fig. 5. As Fig.3, now for Class C galaxies, showing some sign of interaction. Not all these signs may be visible on these small images, and at this particular choice of display levels.

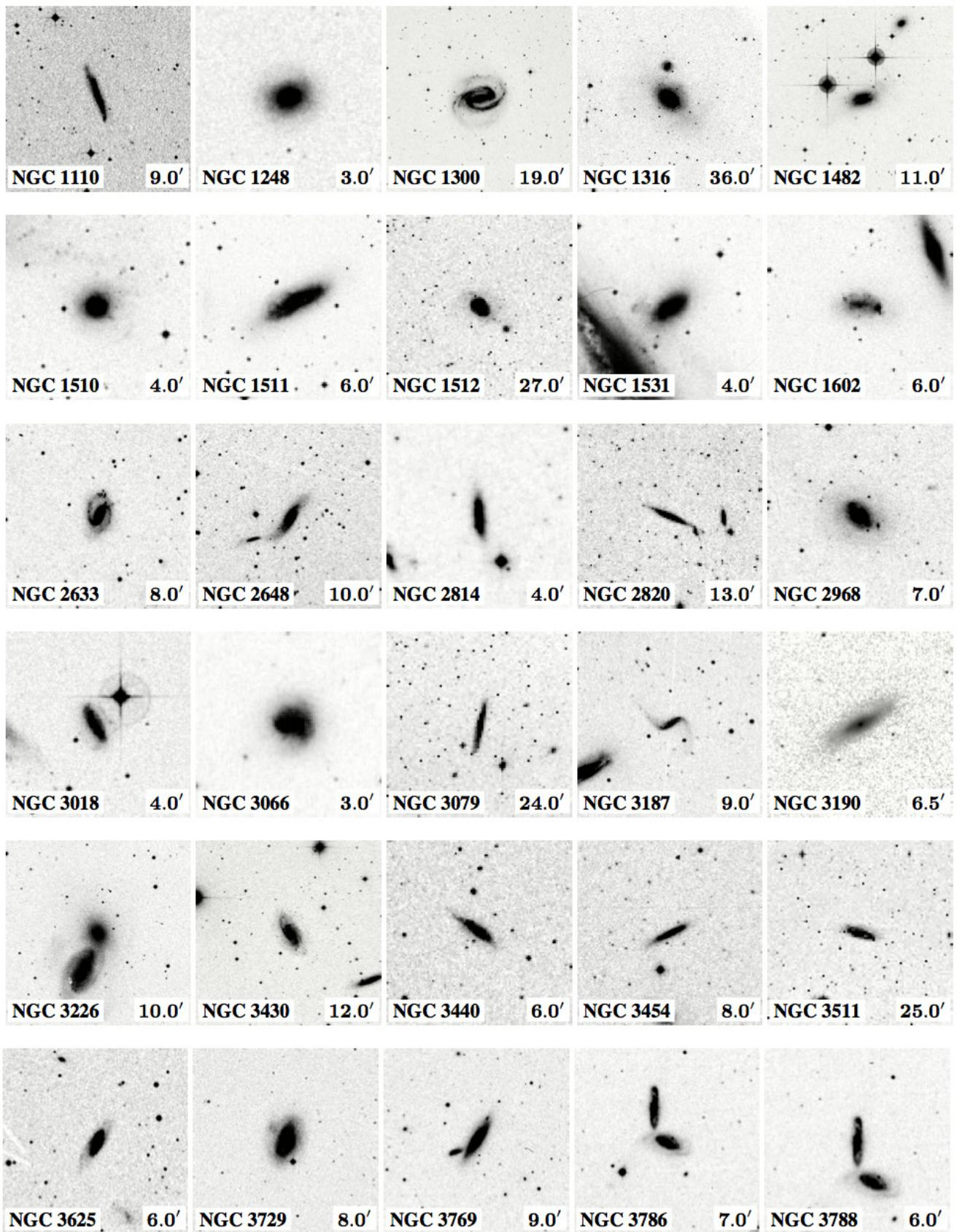
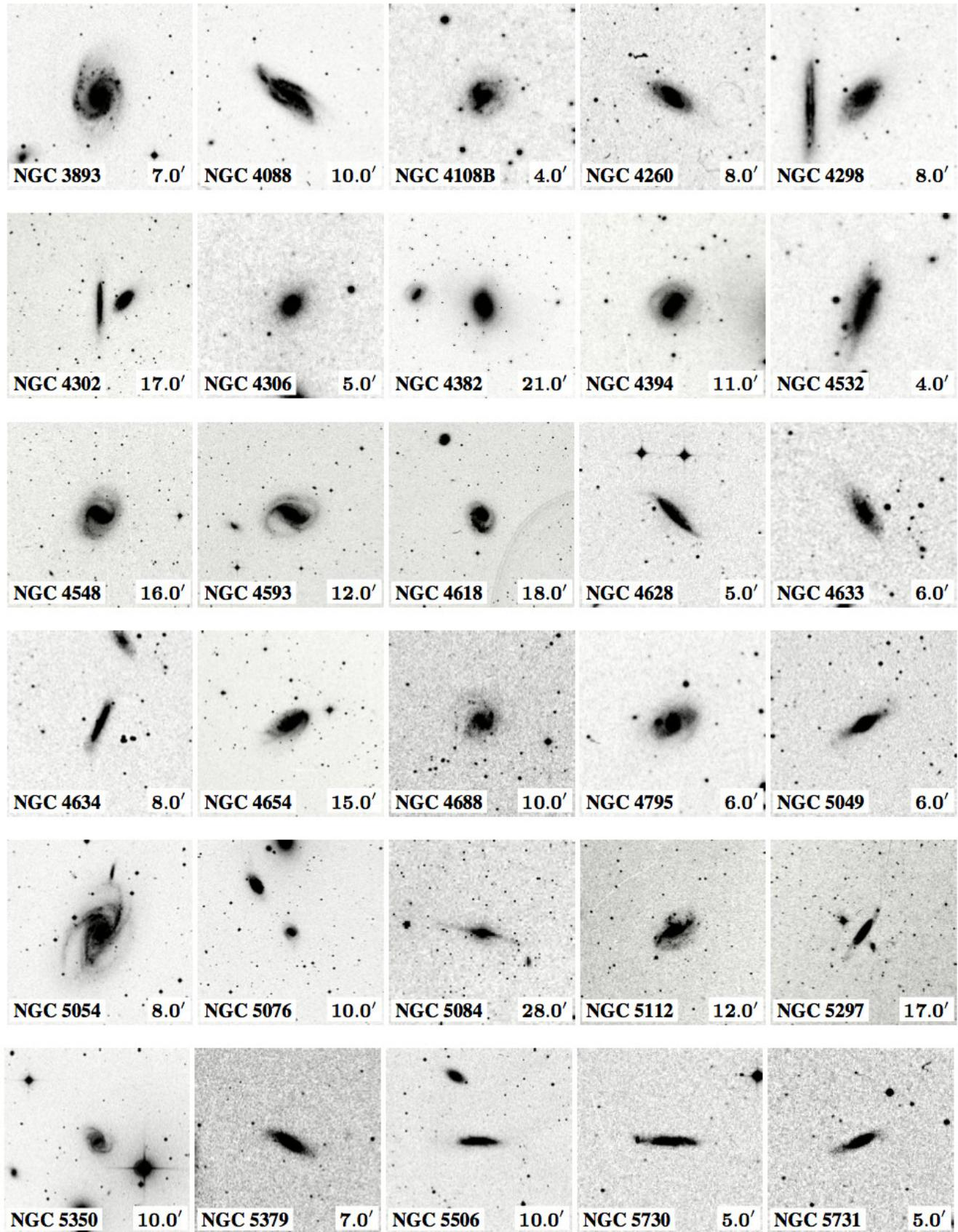


Fig. 5. Continued.

**Fig. 5.** Continued.

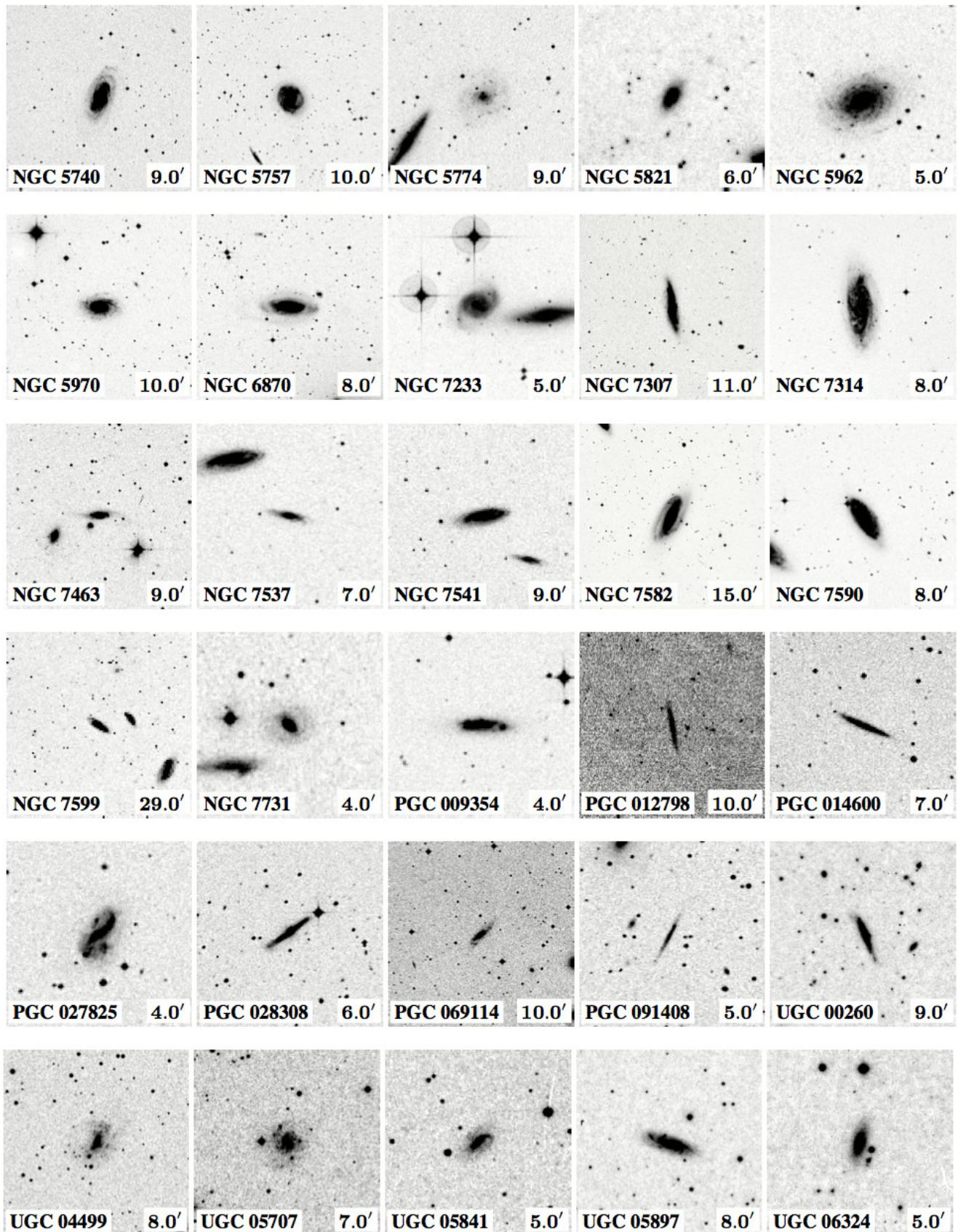


Fig. 5. Continued.

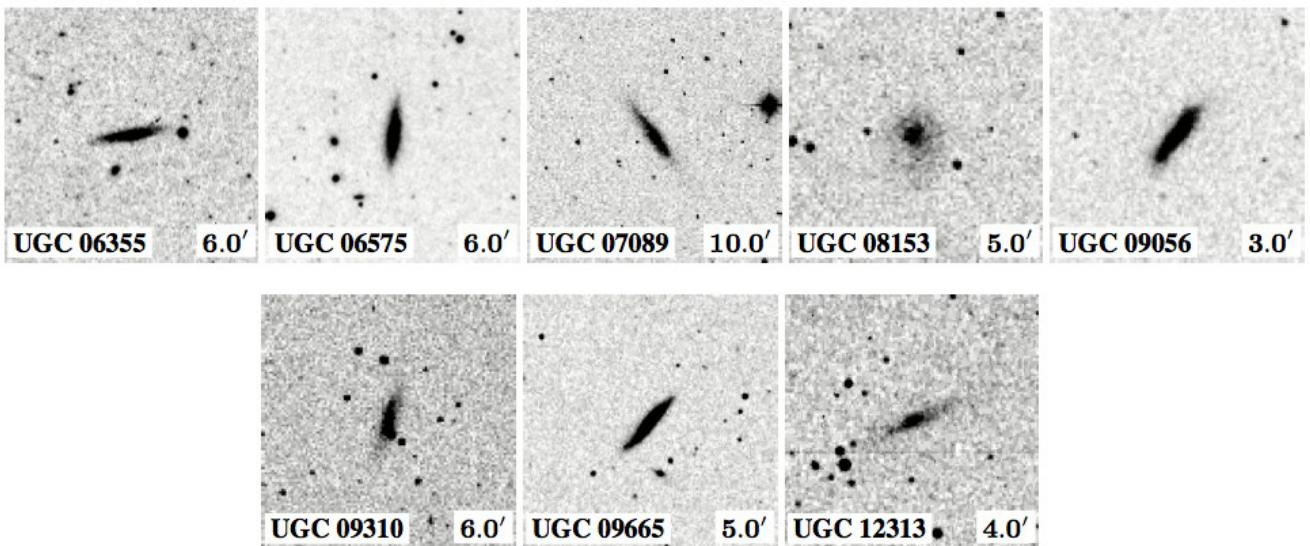


Fig. 5. Continued.

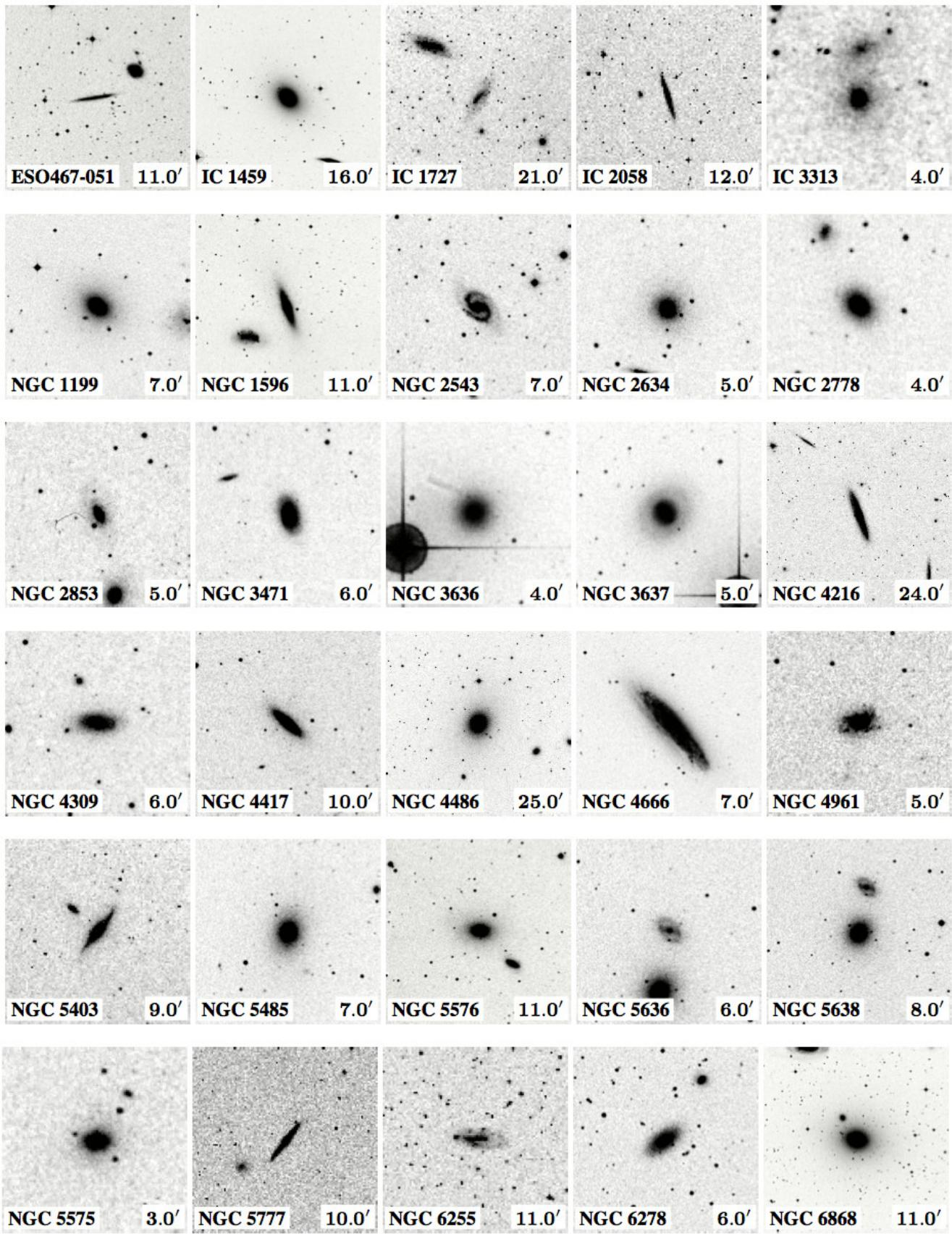


Fig. 6. As Fig.3, now for galaxies with very close companions (closer than 1.5 times the diameter) but which do not show any indication of distorted morphology.

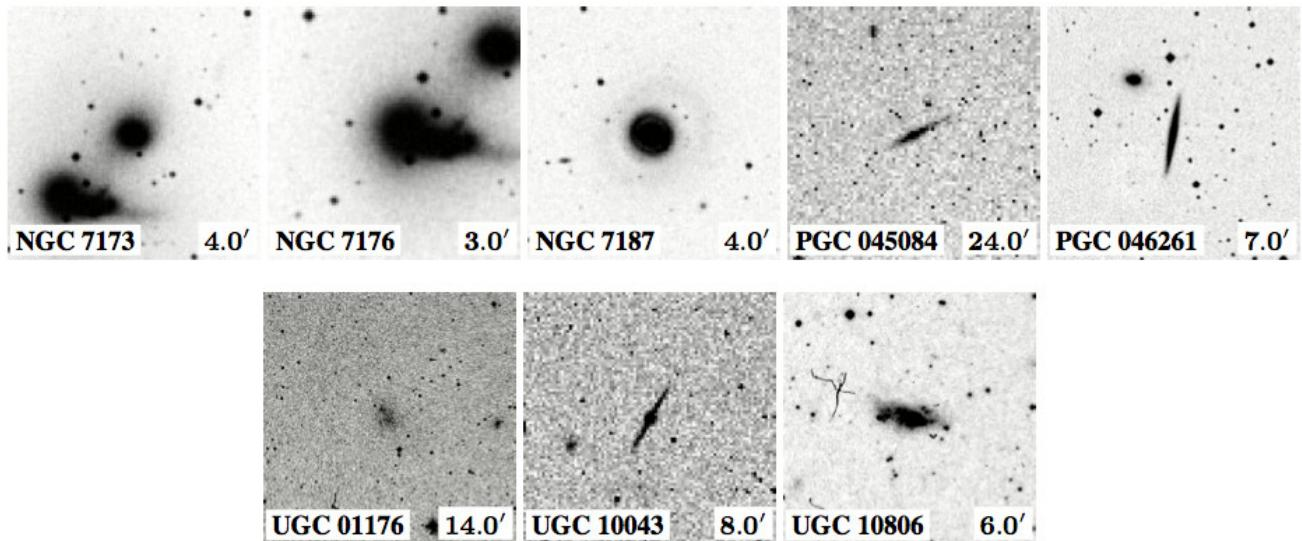


Fig. 6. Continued.